Ph.D. Dissertation in Medical Science

Effect of disease-modifying anti-rheumatic drugs on pathophysiology and clinical course of rheumatoid arthritis-associated interstitial lung disease

항류마티스제제가 류마티스관절염 간질성폐질환의 병리 기전 및 임상경과에 미치는 영향

February 2022

Graduate School of Medicine
Seoul National University
College of Medicine

Sung Hae Chang

Ph.D. Dissertation in Medical Science

Effect of disease-modifying anti-rheumatic drugs on pathophysiology and clinical course of rheumatoid arthritis-associated interstitial lung disease

Submitting a Ph.D. Dissertation in Medical Science

October 2021

Graduate School of Medicine
Seoul National University
College of Medicine
Sung Hae Chang

Confirmation that the Ph.D. Dissertation was written by

Sung Hae Chang

January 2022

Chair	_____(Seal)
Vice-Chair	_____(Seal)
Examiner	_____(Seal)
Examiner	_____(Seal)
Examiner	_____(Seal)

Abstract

Introduction: Rheumatoid arthritis-associated interstitial lung disease (RA-ILD) is one of the pivotal extrapulmonary conditions contributing to increased mortality in rheumatoid arthritis patients. However, the pathophysiology of RA-ILD, including the effect of disease-modifying anti-rheumatoid drugs (DMARDs) is largely unknown.

Objectives: The current study aimed to study the effect of DMARDs on the clinical course of RA-ILD and on the lung microenvironment.

Methods: The clinical course of patients was analyzed using data from the Korean Rheumatoid Arthritis-related Interstitial Lung Disease (KORAIL) cohort, a prospective observational cohort in which patients were followed up and examined annually for three years. Six tertiary medical centers in the Republic of Korea participated in KORAIL cohort. Fibrosis score was defined as the sum of reticular opacity score and traction bronchiectasis/bronchiectasis score on a computed tomography chest scan. Mice of the SKG strain were used as an animal model for RA-ILD. Single-nucleus ribonucleic acid (RNA) sequencing was performed using the lung tissue of SKG mice from four groups: (1) those without zymosan A injection, (2) those injected with zymosan A and treated with phosphate-buffered saline, (3) those injected with zymosan A and treated with methotrexate, and (4) those injected with zymosan A and treated with a tumor necrosis factor α inhibitor (TNFi).

Results: In patients with severe RA-ILD, defined as more than 30% lung involvement, fibrosis score rose significantly in the methotrexate-treated group at the two-year and three-year follow-ups. Histologically evident inflammation was

seen more often in the mice of group 3 (zymosan A injected and methotrexate treated) than in the other groups. Methotrexate treatment heightened transcriptome changes by zymosan A injection in immune cells, fibroblasts, and alveolar epithelial cells, while TNFi treatment alleviated those transcriptome changes, with results resembling those of the mice in group 1 (no zymosan A injection). Interestingly, a unique type II alveolar cell subcluster was seen in the methotrexate-treated mice. This unique cluster was enriched by inflammatory cytokine-responsive genes and showed reduced regenerative capacity.

Conclusion: In the KORAIL cohort, methotrexate administration worsened pulmonary fibrosis in patients with severe RA-ILD. In the mouse model, methotrexate induced severe pneumonia due to the reduced regeneration capacity of type II alveolar cells associated with an inflammatory response.

……

Keywords: Rheumatoid arthritis, interstitial lung disease, single-nucleus RNA sequencing, transcriptome, progressive fibrosing interstitial lung disease, animal disease model, SKG mice

Student Number: 2017-31233

Table of Contents

LIST OF TABLES

LIST OF FIGURES

LIST OF ABBREVIATIONS

ANOVA, analysis of variance

AT1, alveolar type 1

AT2, alveolar type 2

BSA, bovine serum albumin

CCP, cyclic citrullinated peptide

CIA, collagen-induced arthritis

CFA, complete Freud's adjuvant

CPI, composite physiology index

CRP, C-reactive protein

CT, computed tomography

CTD, connective tissue disease

DAPI, 4',6-diamidino-2-phenylindole

DAS, disease activity score

DAS28, Disease Activity Score in 28 Joints

DATP, damage-associated transient progenitor

DEG, differentially expressed genes

DL_{CO}, diffusion capacity for carbon monoxide

DMARDs, disease-modifying antirheumatic drugs

ERA, early rheumatoid arthritis

ESR, erythrocyte sedimentation rate

FVC, forced vital capacity

GAP, gender/age/physiology

GEAR Center, Gyerim Experimental Animal Resource Center

GSEA, gene set enrichment analysis

HAQ-DI, Health Assessment Questionnaire Disability Index

HC, honeycombing

HIER, heat-induced epitope retrieval

HIF1A, hypoxia inducible factor 1A

IFN, interferon

IL-*n*, interleukin-*n*

ILD, interstitial lung disease

IPF, idiopathic pulmonary fibrosis

IQR, interquartile range

IRF1, interferon regulatory factor 1

JAK, Janus kinase

KORAIL cohort, KOrean Rheumatoid Arthritis Interstitial Lung disease cohort

KRAS, Kirsten rat sarcoma viral oncogene homolog

LDA, low disease activity

LINCS, Library of Integrated Network-Based Cellular Signatures

LRA, long-standing rheumatoid arthritis

MHC, major histocompatibility complex

mRNA, messenger RNA

MSigDB, The Molecular Signatures Database

MTX, methotrexate

NES cell, neuroepithelial-like stem cell

NGS, next-generation sequencing

NK, natural killer

PBS, phosphate-buffered saline

PBST, phosphate-buffered saline solution with Tween 20 or Triton X100

PFT, pulmonary function test

PGA, patients' global assessment

PMN, polymorphonuclear

RA, rheumatoid arthritis

RA-ILD, rheumatoid arthritis-associated interstitial lung disease

RF, rheumatoid factor

RNA, ribonucleic acid

RO, reticular opacity

SD, standard deviation

scRNA seq, single-cell RNA sequencing

SJC, swollen joint count

snRNA seq, single-nucleus RNA sequencing

SMA, smooth muscle actin

SPF, specific-pathogen free

STAT*n*, signal transducer and activator of transcription *n*

TB, traction bronchiectasis/bronchiolectasis

TGF, transforming growth factor

TJC, tender joint count

TNF, tumor necrosis factor

UIP, usual interstitial pneumonia

UMI, unique molecular identifier

UMAP, Uniform Manifold Approximation and Projection

UV, ultraviolet

ZyA, zymosan A

INTRODUCTION

1.1. Study Background

Recent progress in knowledge and treatment of rheumatoid arthritis

Rheumatoid arthritis (RA) is the prevalent chronic inflammatory arthritis, with a worldwide prevalence of about 5 per 1000 adults[1]. If not adequately controlled, chronic inflammation in RA causes irreversible joint damage that results in severe disability. In addition, chronic inflammation leads to extra-articular manifestations, such as rheumatoid vasculitis, and various comorbidities such as cardiovascular disease or malignancies.

In recent years there has been a leap in genetic and pathogenic insights into RA.[2] The discovery of autoantibodies against post-transcription-modified peptides, such as citrullinated peptides, has aided in early diagnosis via revision of classification criteria. The evolving pathophysiology has made progress in new drugs, such as biologics or targeted synthetic disease-modifying antirheumatic drugs (DMARDs), with high efficacy and fewer toxicities. Increased treatment options enable treat-to-target strategies. As a result, during the period 2000 to 2010, there was a twofold increase in 6-month remission rates and consistent improvement in other disease activity measures. All-cause mortality has improved even more.

The burden of rheumatoid arthritis-associated lung disease

However, this remarkable progress does not apply to a specific group of patients with RA, namely those with extra-articular RA manifestations.[3] Rheumatoid arthritis involves primarily synovial joints, but, because it is a systemic autoimmune disease, it affects various other organs. The extra-articular manifestations are classified as

severe (vasculitis, interstitial lung disease, Felty's syndrome, pericarditis, pleuritis, scleritis) or less severe (rheumatoid nodules and secondary Sjogren syndrome). With improved treatment, the incidence of some extra-articular manifestations such as vasculitis has lessened, whereas other manifestations such as interstitial lung disease are unchanged. Although mortality in the same cohort has declined over time, extra-articular manifestations are occurring twice as often as premature mortality.[3, 4]

Lung disease is one of these manifestations contributing greatly to morbidity and mortality. It can affect almost every lung compartment, including the large and small airways, pleura, pulmonary vessels, and lung parenchyma.[5, 6] More than half of RA patients are estimated to have lung manifestations during the course of the disease. The most challenging lung manifestation is interstitial lung disease (ILD); a population-based study has shown the probability of death to be about ten times higher in patients with RA-associated interstitial lung disease (RA-ILD) than in those without ILD, even in the current biologic era.[3, 7]

The unknowns of RA-ILD

The actual incidence of RA-ILD is unknown, but it is estimated that 5-17% of RA patients show symptoms and up to 30% present with radiographically evident ILD.[7-11] That wide variability is due to timing and methods of diagnosis. Because in most cases respiratory symptoms develop only after the onset of joint symptoms and because it is not standard practice to evaluate computed tomography (CT) chest scans at the time of diagnosis, diagnosis of ILD in patients with RA is often delayed. The course of RA-ILD is also mostly unknown, but some patients suffer rapid progression with deteriorating pulmonary function.[12-14] Several factors are associated

with increased mortality: older age, a history of having ever smoked, a 10% decline in predicted forced vital capacity (FVC), or a radiographic pattern of usual interstitial pneumonia (UIP).

Recent clinical trials of antifibrotic agents in ILD provide integrative insights to identify a group of ILD patients with a progressive phenotype experience that in clinical course resembles idiopathic pulmonary fibrosis (IPF) regardless of clinical diagnosis.[12] This concept is important because emerging evidence clearly shows the benefit of antifibrotic agents in improving survival in patients with IPF. Patients with progressive fibrosing ILD may also benefit from this therapy. However, it is still unclear how many patients have progressive fibrosis, how fast those progressions occur, and what causes those progressions.

Of note, unlike other connective tissue diseases where the activity is assessed and treated organ by organ, RA activity is evaluated according to affected joints and the treatment mainly addresses arthritis.[15, 16] The current standard of care for RA advocates a treat-to-target strategy, targeting clinical remission based on arthritis activity and recommending early treatment with methotrexate as a first-line cornerstone drug. Those principles have accomplished a decline in mortality and disability due to arthritis. However, there are very few data on how controlling arthritis activity affects lung function or progression of lung fibrosis; it is also unknown what effect DMARDs have on the progression of lung disease.[9, 17, 18] There is debate on whether methotrexate, despite being the cornerstone drug for RA, is safe in RA patients with lung involvement.[18-20]

Need for an animal model of RA-ILD

Pathology and tissue samples are valuable not only in diagnosis but also in understanding the pathophysiology of disease and further insight for new treatment development. For example, the meticulous observation and discovery of T-cell infiltrations around cancer tissue has led to the current progress in immune-oncologic treatment, including chimeric antigen receptor T-cell therapy or cytotoxic T-lymphocyte-associated protein-4 immunoglobulin agnostic treatment. In the same context, to understand RA-ILD's pathophysiology and address the effect of DMARDs on the lung, it is necessary to analyze lung tissue of patients with RA-ILD. However, such tissue samples are and will continue to be challenging to obtain because lung biopsy is not needed for either diagnosis or prognosis, due to sophisticated CT scans.

Therefore, an animal model for RA-ILD is an option, but few animal models develop both arthritis and ILD. There are several animal models for arthritis, but only three develop lung disease[21]; the tumor necrosis factor-transgenic model, the adjuvant arthritis model, and the SKG mouse. One specific line of TNF-transgenic mice (the 3647 line), which systemically overexpresses TNF, is known to develop arthritis within 4 to 8 weeks of age, showing severe lung disease similar to human ILD.[21] In the adjuvant arthritis model, injection of complete Freud's adjuvant (CFA) and mycobacterium antigen or synthetic adjuvant propanediamine to certain strains of rat results in arthritis and pneumonitis.[22, 23] Finally, SKG mice develop not arthritis and pneumonitis with environmental triggering such as β-glucan in the genetic background of Zap-70 point-mutation; this is very similar to the onset of autoimmune diseases in humans.

Although there are differences between mice and humans, in RAILD, where it is difficult to obtain human pathological tissues, these disease animal models are very useful for studying the pathophysiology of diseases and the effects of medication on the pathophysiology. Therefore, to study the effect of DMARDs, we investigated not only the clinical course of RA-ILD using patients' cohort but also on the lung microenvironment using SKG mice as a disease animal model.

1.2. Purpose of Research

The current study was conducted with the following goals:

1. Establish an animal model of RA-ILD
2. Define the pathologic mechanism of RA-ILD using transcriptome analysis
3. Explore the changes in those pathologic mechanisms with treatment
4. Describe the course of RA-ILD in a prospective cohort
5. Determine the effect of DMARDs on the course of RA-ILD in a prospective cohort.

Part I. Clinical outcomes analysis to explore the effect of disease-modifying antirheumatic drugs on the lung of rheumatoid arthritis-associated lung disease using a prospective cohort

Introduction

ILD is a disease with a highly heterogeneous clinical course across different ILD subgroups and often within the same ILD subgroup[13, 24]. Nevertheless, a variable proportion of patients within each ILD subgroup exhibit a similar clinical progressive phenotype characterized by persistently deteriorating pulmonary function, respiratory symptoms, and fibrosis. Recent clinical trials have demonstrated that the antifibrotic drugs pirfenidone and nintedanib significantly slow such a progression in patients with ILD other than idiopathic pulmonary fibrosis (IPF)[25]. However, as this study mainly included patients with stable connective tissue diseases (CTD), RA activity was not considered. Furthermore, limited data regarding outcomes of patients with RA-ILD with a progressive phenotype. In the beginning, patients with RA visit physicians because of arthritis, and they are treated with DMARDs.

Herein, we evaluated the relationship between RA disease activity and lung physiology in patients with RA-ILD. In addition, we analyzed subgroups according to methotrexate treatment or not.

Materials and methods

Study design

The Korean Rheumatoid Arthritis Interstitial Lung disease (KORAIL) cohort is a multicenter prospective observational cohort study conducted to assess the course of RA-ILD. The ethical committees of each participating center approved the study protocol and procedures (Daegu Catholic University Medical Center: CR-15-009, Kyung Hee University Hospital: 2016-11-063, Seoul National University Hospital: 1407-027-592, Seoul National University Bundang Hospital: B-1412-280-412, Yonsei University Severance Hospital: 2014-2417-002, Soonchunhyang University Cheonan Hospital: 2016-01-008). All patients provided informed consent, and all procedures followed the ethical standards outlined in the Declaration of Helsinki and Good Clinical Practice guidelines.

Patient recruitment

Patients aged 18 years or more who regularly attended an outpatient rheumatology clinic were recruited into the cohort. Patients were enrolled if they were diagnosed with RA according to the 2010 American College of Rheumatology/European League Against Rheumatism RA classification criteria and were clinically diagnosed with ILD based on chest CT or lung biopsy findings regardless of their respiratory symptoms. The study began in January 2015, and patient recruitment ended in December 2018. Enrolled patients were followed yearly since enrollment. This study was an interim analysis of data from patients who had completed a two-year follow-up or died as of January 2021.

Data collection

The following items were evaluated annually: body weight; height; smoking and drinking history; pulmonary function tests (PFTs), including FVC and diffusion capacity for carbon monoxide (DL_{CO}); chest CT; radiographs of the chest, hands, and feet; and laboratory test results, including C-reactive protein (CRP) levels and erythrocyte sedimentation rate (ESR). We also surveyed current RA medications, including steroids and any DMARDs. Data from all six participating medical centers were collected using an electronic case report form (http://61.78.63.84:8080/ecrf). Among the entire cohort of patients, those who had ever been treated with methotrexate for 24 weeks or more were analyzed to assess the effect of methotrexate on the course of RA-ILD.

ILD diagnosis and definition of ILD progression

At baseline, patients were screened and enrolled based on the assessment of CT scans by expert radiologists at each medical center. After that, images were independently reviewed by two expert radiologists who were blinded to patients' clinical status and demographics. Pulmonary physiology was assessed annually, and ILD progression was determined based on FVC changes combined with DL_{CO} changes. Progression of ILD was defined by either an FVC decline of $\geq$10% or an FVC decline of 5–10% combined with a DL_{CO} decline of $\geq$15%.

Chest CT image scoring system

Two independent radiologists reassessed CT scans, scoring them on the extent of pure ground-glass opacity (GGO), reticular opacity, traction

bronchiectasis/bronchiolectasis, honeycombing, and emphysema adapted from the Scleroderma Lung Study scoring system.[26] The extent of total interstitial lung abnormalities (ILAs) was also evaluated. For our study, we defined lung fibrosis on CT scans in two ways: fibrosis A is defined as the presence of reticular opacity together with traction bronchiectasis/bronchiolectasis, and fibrosis B is defined as the presence of honeycombing or the presence of fibrosis A regardless of honeycombing.

RA disease activity measurement

At baseline and at each visit we collected the following clinical characteristics: 28-joint counts of swollen and tender joints (SJC28 and TJC28), patient global assessment score, and Health Assessment Questionnaire Disability Index (HAQ-DI) score. The treating rheumatologist assessed the swollen and tender joints. Disease activity was categorized as remission (score $\leq$2.6), low disease activity (score >2.6 and $\leq$3.2), moderate disease activity (score >3.2 and $\leq$5.1), or high disease activity (score >5.2) based on the Disease Activity Score in 28 Joints (DAS28) with ESR (DAS28-ESR) or DAS28 with CRP (DAS28-CRP).

Definition of patients with methotrexate treatment

To analyze the effect of methotrexate treatment on the course of ILD, we selected patients who were treated with methotrexate for at least 24 weeks during the follow-up periods.

Statistical analysis

Data were summarized using descriptive statistics. We performed between-group comparisons using the chi-squared test and Fisher's exact test, comparisons among ≥3 groups using analysis of variance (ANOVA), and further multiple comparisons using Fisher's exact test with Bonferroni adjustment or Tukey's multiple comparison method. To analyze changes in pulmonary physiology over time, we applied linear mixed-effects models, allowing separate fits for subjects. We did not correct linear mixed-effects model analysis with age or gender because the velocity of change was of concern. The same model was used for analyses among patients, with the slope of the FVC decline calculated for each patient and with the average values compared between patients with methotrexate and those without methotrexate. Analyses associated with pulmonary physiology measurements included all patients with results for at least two PFTs during their second visit after enrollment, regardless of survival. All data were analyzed using SAS statistical analysis software (v 9.1; SAS Institute, Inc., Cary, NC, USA).

Results

Demographic characteristics

Since patient enrollment began in January 2015, a total of 168 patients have been included in this cohort. Up to January 2021 20 patients (12.2%) had died and 31 (18.5%) were lost to follow-up such that their survival could not be confirmed. Eight patients were excluded because of no CT chest scan abnormalities after reevaluation of their scans by the radiologists in the current study (Figure 1). Clinical characteristics of the entire cohort are detailed in Table 1.

ILD was diagnosed at least six months after RA diagnosis in 94 patients (57.7%) and at least six months before RA diagnosis in only ten patients (6.1%). In 59 patients (36.2%), RA and ILD were concomitantly diagnosed within a 6-month period (n=8, 4.9%), RA was diagnosed before ILD (n=33, 20.2%), or ILD was diagnosed before RA (n=18, 11.0%).

Among 160 patients, 101 had not been treated with any biologic DMARDs or targeted-synthetic DMARDs. Thirty-two patients had ever been treated with methotrexate for at least 24 weeks during the study period (the“MTX”group), and 69 had not (the“no-MTX”group). We analyzed 101 patients because the current study aimed to investigate the effect of methotrexate on the lung.

Both groups' mean age and body mass index (BMI) were comparable (Table 2). The proportion of smokers and gender distribution were also comparable. Eighty percent of the patients were positive for both rheumatoid factor (RF) and anti-cyclic citrullinated peptide (anti-CCP) antibodies. All patients in the methotrexate-treated

group were positive for anti-CCP antibody, of whom four patients (12.5%) were negative for RF.

RA disease activity

At the three-year follow-up, overall composite disease activity scores, including DAS28-ESR and DAS28-CRP, were significantly improved in the entire cohort (Figure 2). Tender joint count and swollen joint count improved compared with the baseline, but laboratory examinations such as ESR and CRP, patients' global assessment, and health-associated questionnaire scores were not significantly improved (Table 3). However, the two groups' disease activity measurements were comparable during follow-up periods.

Pulmonary function test

At enrollment, the mean FVC and the mean percentage of predicted (% predicted) FVC was comparable between the two groups (Table 4). At the three-year follow-up, annual decline in FVC (ml) was comparable (-43.9 ml/year, -60.9 - -26.9 in the MTX group versus -50.1 ml/year, -63.4, -36.8 in the no-MTX group, p=0.58, Figure 3). Twenty-eight percent of patients exhibited a relative decline of $\geq$10% in the % predicted FVC from baseline in the MTX group versus 37% in the no-MTX group (p=0.37). The mean of % DL_{CO} predicted was comparable between the groups. The proportion of patients who experienced a 15% or more decline in % DL_{CO} from baseline was also comparable.

Interstitial lung abnormality change on CT scan

The most frequently observed interstitial lung abnormality (ILA) on chest CT was reticular opacity (Table 5). Honeycombing was observed in 60.4% of patients. About 40% showed >10% extent of ILA, and 18.8% showed ≥ 30% extent. Eighty-five percent of patients exhibited lung fibrosis A and 95.1% did fibrosis B. Among patients with >10% involvement of ILA, lung fibrosis B was observed in 37.6 % of them. The extent of ILA involvement, the proportion of patients with lung fibrosis, and honeycombing were comparable between the groups.

Of note, among patients with lung involvement more than 30%, their fibrosis A scores, sum of reticular opacity, and traction bronchiectasis/bronchiolectasis were significantly higher if they'd had methotrexate treatment (Table 5, Figure 4).

Discussion

In the current study, methotrexate treatment did not affect pulmonary physiology or fibrosis progression on CT in the overall cohort. However, treatment with methotrexate was associated with worsening traction bronchiectasis/ bronchiolectasis and honeycombing among patients with extensive pneumonitis.

Methotrexate-associated pneumonitis can be classified into three categories clinically, apart from infectious pneumonia related to methotrexate treatment: (1) pneumonitis caused by methotrexate itself, (2) newly developed pneumonitis in patients with unknown history of RA-ILD, and (3) pneumonitis worsened by methotrexate treatment in patients with RA-ILD.

The first category, pneumonitis caused by methotrexate, belongs to hypersensitivity pneumonitis. It is an infrequent drug-related reaction in fewer than 1% of RA patients starting methotrexate.[19] Clinical symptoms are nonspecific, such as shortness of breath, dry cough, hypoxia, or fever without evidence of infection. Chest CT shows diffuse bilateral GGO changes. Most cases improve with discontinuation of the drug, and empirical steroid administration helps to ease clinical symptoms. Still, delayed recognition might result in devastating consequences, with a high mortality rate of up to 20%.

Regarding the second category, there are controversies as to whether methotrexate induces ILD.[19, 27, 28] In particular, if a patient has already been treated with methotrexate for arthritis diagnosed with ILD, it is difficult to distinguish whether the ILD is associated with methotrexate treatment or was preexisting and ignored, because the current standard of care does not support routine screening for ILD in patients diagnosed with RA. Nevertheless, since methotrexate has been widely used

as background medication in many clinical trials, data from those trials help us to infer the answer to the issue. In a meta-analysis of results of randomized clinical trials (RCTs) performed on patients with psoriatic arthritis, psoriasis, or inflammatory bowel disease, methotrexate was not associated with respiratory events. [29]In contrast, in a meta-analysis of RCTs with RA patients, who have an intrinsic risk of developing ILD, methotrexate treatment showed a significant increase in all adverse respiratory events, mainly due to respiratory infection. [30]According to the latter study, when including limited studies that described pneumonitis, the risk of "pneumonitis" was higher with methotrexate. However, all studies describing "pneumonitis" were in the early 2000s, and patients with preexisting lung involvement were not excluded, unlike those that excluded patients with definite lung involvement. Recently a large-scale RCT of methotrexate (15-20 mg per week) and placebo cardiovascular inflammation reduction was performed on nearly 4500 patients.[31, 32] In that study, severe pulmonary events or pneumonitis rarely occurred; the severe pulmonary adverse event was 0.5% in the methotrexate group and 0.3% in the placebo group, and possible pneumonitis was 0.3% (n=7) in the methotrexate group and <0.1% (n=1) in the placebo group.[31] Considering the current data from RCTs, the risk of *de novo* development of ILD is very low in patients without intrinsic ILD risk.

Finally, it is controversial whether methotrexate worsens pneumonitis in patients with preexisting ILD. The mortality risk has been shown to be higher in patients with a UIP pattern or fibrosing pattern in high-resolution CT (HRCT), lower baseline % predicted FVC, a 10% decline from baseline in % predicted FVC , older age, male sex, a history of smoking, a lower % predicted DL_{CO}, a higher composite

physiological index (CPI), or a higher gender-age-physiology (GAP) stage.[33-37] Regarding treatment, one study showed that conventional synthetic DMARDs had no impact while TNFα inhibitors increased all-cause mortality, whereas rituximab or mycophenolate mofetil decreased all-cause mortality.[37] A study related to methotrexate has shown that methotrexate treatment, as well as old age and UIP patterns, were significant risk factors for acute exacerbation of RA-ILD.[38] In contrast, another study concluded that UIP pattern and non-use of methotrexate was a poor prognosis factor and was associated with acute exacerbation.[39]

Notably, almost all studies of the three categories were retrospective except RCTs. A CT image is essential for diagnosis of ILD. In standard care, however, a chest CT scan is not recommended as a part of the initial workup at the time of RA diagnosis. Usually, a chest CT scan is executed when dyspnea has developed. Therefore, most studies belonging to the second category have analyzed the effect of methotrexate on the incidence of ILD. Most studies of the third category, investigating the impact of methotrexate on patients with preexisting ILD, were mainly concerned with mortality or acute exacerbation of ILD. Therefore, from the results of the studies so far, it is challenging to know the impact of treatment on the long-term landscape of RA-ILD.

To further understand the effect of methotrexate on the lungs in an aspect of the mechanism of action beyond clinical consequence, the author conducted additional experiments to elucidate the pathophysiology of methotrexate on the lungs using a mouse model. These experiments are described in Part II.

Figure 1. Enrollment and follow-up in overall populations of the KORAIL cohort

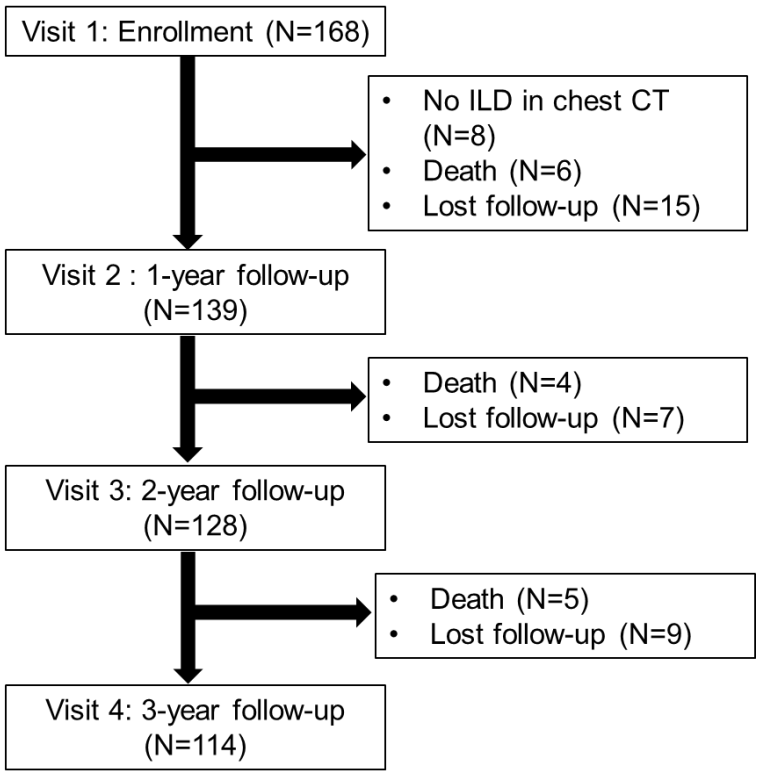

Table 1. Clinical characteristics of the entire KORAIL cohort at enrollment

Characteristic	Number (%)
Number of patients	163
Age at enrollment (years), mean (SD)	66.4 (8.1)
≥65 years, n (%)	96 (58.9)
≥70 years, n (%)	57 (35.0)
≥75 years, n (%)	23 (14.1)
Sex, n (%)	
Male	54 (33.1)
Female	109 (66.9)
RA duration (years), median (IQR)	5.9 (9.3)
ILD duration (years), median (IQR)	1.6 (4.3)
BMI, mean (SD)	23.7 (3.2)
Smoking status, n (%)	
Never a smoker	119 (73.0)
Ex-smoker	28 (17.2)
Pack-years, median (IQR)	30.0 (17.5)
Current smoker	15 (9.2)
Pack-years, median (IQR)	24.0 (1.0–55.0, 14.0)
Unknown	1 (0.6)
RA medications at enrollment	
Methotrexate, n (%)	100 (61.3)
Glucocorticoid, n (%)	160 (98.2)
Biologic DMARDs, n (%)	60 (36.8)
RF positivity, n (%)	143 (87.7)
Titer, mean (SD)	279.5 (513.6)
Anti-CCP antibody positivity*, n (%)	154 (94.5)
≥200	76 (52.4)
Titer, mean (SD)	279.8 (266.7)

*ILD was diagnosed based on chest CT scan or lung biopsy.

Table 2. Clinical characteristics of patients without biologic DMARDs at enrollment: methotrexate versus no methotrexate

Characteristic	Total	Methotrexate	No methotrexate	P-value
Number of patients	101	32	69	
Age at enrollment (mean ± SD, years)	67.1±7.8	65.7±8.4	67.7±7.5	0.22
Female, n (%)	67 (66.3)	25 (78.1)	42 (60.9)	0.09
RA Duration (mean ± SD, years)	6.7±8.0	6.8±8.8	6.6±7.6	0.86
ILD Duration* (mean ± SD, years)	2.4±3.0	2.5±3.4	2.3±2.8	0.78
BMI, mean ± SD	23.5±3.1	23.2±2.9	23.6±3.2	0.52
Smoking, n (%)				0.61
Never a smoker	73 (72.3)	25 (78.1)	48 (69.6)	
Ex-smoker	18 (17.8)	4 (12.5)	14 (20.3)	
Current smoker	10 (9.9)	3 (9.4)	7 (10.1)	
RF positive, n (%)	89 (88.1)	28 (87.5)	61 (88.4)	1.00
Titer, mean ± SD	253.7±458.9	227.3±278.8	265.9±522.9	0.79
Anti-CCP positive*, n (%)	94 (93.1)	32 (100.0)	62 (89.9)	0.09
Titer, mean ± SD	280.0±280.2	278.5±278.1	280.7±283.8	0.73

*ILD was diagnosed based on chest CT scan or lung biopsy.

Table 3. Rheumatoid arthritis disease activity of patients without biologic DMARDs at follow-ups: methotrexate versus no methotrexate

	At enrollment (V1)		1-year follow-up (V2)		2-year follow-up (V3)		3-year follow-up (V4)		P**
	MTX	No MTX	MTX	No MTX	MTX	No MTX	MTX	No MTX	
Tender joint count	2.2 ± 3.6	3.3 ± 5.0	1.0 ± 1.6	1.6 ± 3.1*	0.2 ± 0.7*	1.5 ± 3.4*	0.6 ± 1.2	1.7 ± 3.3*	0.78
Swollen joint count	1.6 ± 2.2	2.6 ± 3.2	1.3 ± 2.0	1.3 ± 2.9*	0.5 ± 0.9	1.7 ± 3.2*	0.9 ± 2.1	1.4 ± 3.1*	0.43
PGA (0-100)	35.2 ± 28.3	33.9 ± 28.5	29.2 ± 23.6	18.7 ± 19.9*	25.2 ± 19.7	28.5 ± 28.3	27.3 ± 22.2	29.4 ± 28.1	0.26
ESR, mm/hr	43.4 ± 26.9	38.3 ± 26.0	35.9 ± 24.8	28.6 ± 21.5*	33.2 ± 25.1*	37.4 ± 24.4	33.1 ± 21.1	31.7 ± 24.5	0.19
CRP, mg/dl	10.0 ± 14.0	10.3 ± 15.6	7.9 ± 9.5	5.3 ± 9.1	9.0 ± 17.5	16.9 ± 40.1	7.7 ± 11.5	8.9 ± 16.3	0.36
DAS28-ESR	3.7 ± 1.4	3.9 ± 1.4	3.3 ± 1.3	3.0 ± 1.2	2.8 ± 0.7*	3.4 ± 1.4*	3.0 ± 0.9*	3.2 ± 1.3*	0.17
DAS28-CRP	2.9 ± 1.3	3.1 ± 1.4	2.5 ± 1.0	2.3 ± 1.0*	2.0 ± 0.7*	2.6 ± 1.4*	2.3 ± 0.8*	2.5 ± 1.3*	0.10
HAQ-DI score	0.58 ± 0.60	0.71 ± 0.86	0.49 ± 0.51	0.59 ± 0.86	0.60 ± 0.84	0.81 ± 1.02	0.66 ± 0.84	0.84 ± 1.01	0.95
Boolean remission	31 (96.9)	65 (94.2)	23 (92.0)	50 (89.3)	24 (96.0)	43 (84.3)	20 (100.0)	41 (100.0)	0.70

*P<0.05 compared with baseline

**P-value was calculated by linear mixed-effects ordinal or binary logistic regression with random intercept model for repeated measures analysis to show the interaction effect between visit and group.

Figure 2. Index-based rheumatoid arthritis disease activity of patients without biologic DMARDs during follow-up: methotrexate versus no methotrexate.

A. Disease activity score change and B. proportion of disease activity using Disease Activity Score in 28 Joints with ESR (DAS28-ESR)

A.

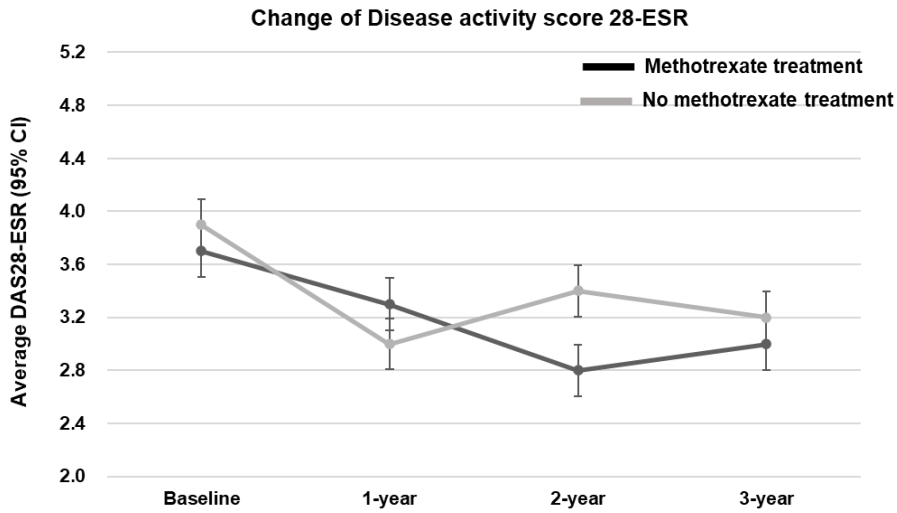

B.

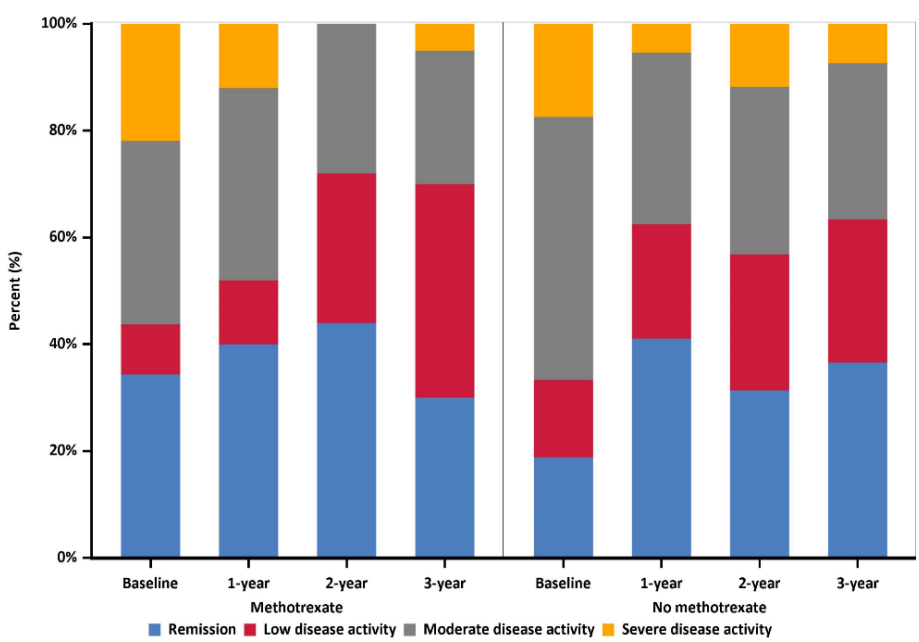

Table 4. Pulmonary physiology changes without biologic DMARDs during follow-up: methotrexate versus no methotrexate

Characteristic	Total	Methotrexate	No methotrexate	P-value
Number of patients	36	12	24	
Forced vital capacity (FVC)				
FVC (mL), mean ± SD: baseline	2242.8±632.2	2183.3±675.7	2272.5±622.1	0.70
% FVC predicted (%), mean ± SD: baseline	76.8±15.3	77.3±16.5	76.5±15.0	0.89
Annual rate of change in FVC (ml), mean (95% CI)	-54.4 (-73.3 - -35.4)	-38.2 (-64.6 - -11.8)	-62.4 (-88.3 - -36.6)	0.23
Patients with a relative ≥10% decline from baseline in % FVC predicted, n (%)	16 (44.4)	5 (41.7)	11 (45.8)	0.81
Patients with a relative ≥10% decline from baseline in FVC ml, n (%)	19 (52.8)	5 (41.7)	14 (58.3)	0.35
Diffusing capacity (DL_{CO})				
DL_{CO} predicted (%), mean ± SD: baseline	63.9±20.5	64.6±25.6	63.6±17.9	0.89
Patients with a relative ≥15% decline from baseline in DL_{CO} predicted, n (%)	21 (60.0)	8 (66.7)	13 (56.5)	0.72
Progressive ILD				
A. Patients with a relative ≥10% decline from baseline in % FVC predicted, n (%)	16 (44.4)	5 (41.7)	11 (45.8)	0.81
B. Patients with a relative ≥5% to <10% decline from baseline in % FVC predicted and a ≥15% decline from baseline in DL_{CO} predicted, n (%)	23 (63.9)	9 (75.0)	14 (58.3)	0.47
A + B	28 (77.8)	10 (83.3)	18 (75.0)	0.69

Figure 3. Annual rates of decline and change from baseline over time in forced vital capacity and diffusion capacity: methotrexate versus no methotrexate.

A. Annual rates of change in (a) FVC (mL/year) during three years of follow-up. B. Changes in mean annual FVC (ml). C. Changes in mean annual percent of predicted DL_{CO}.

A.

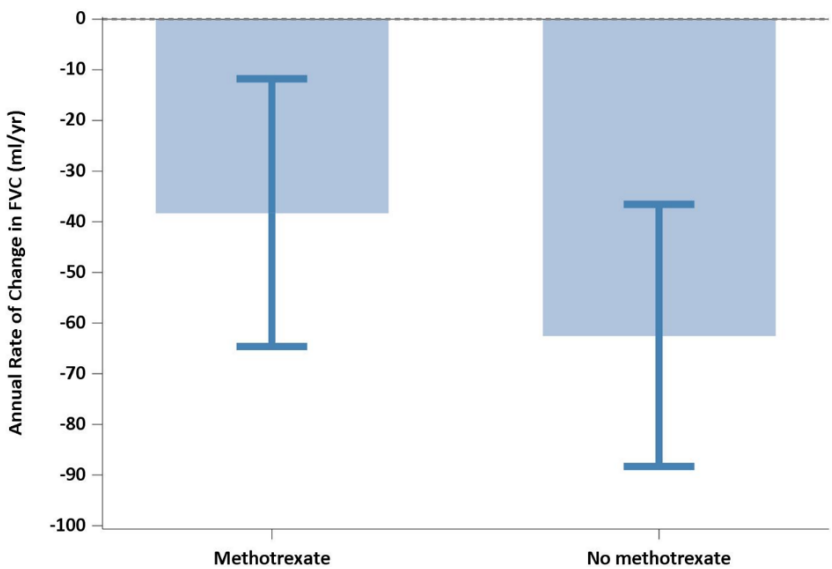

B.

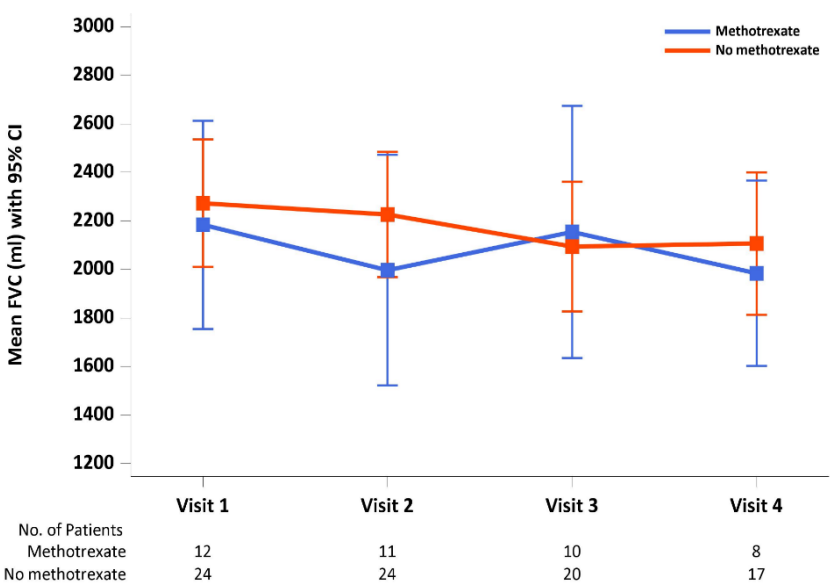

C.

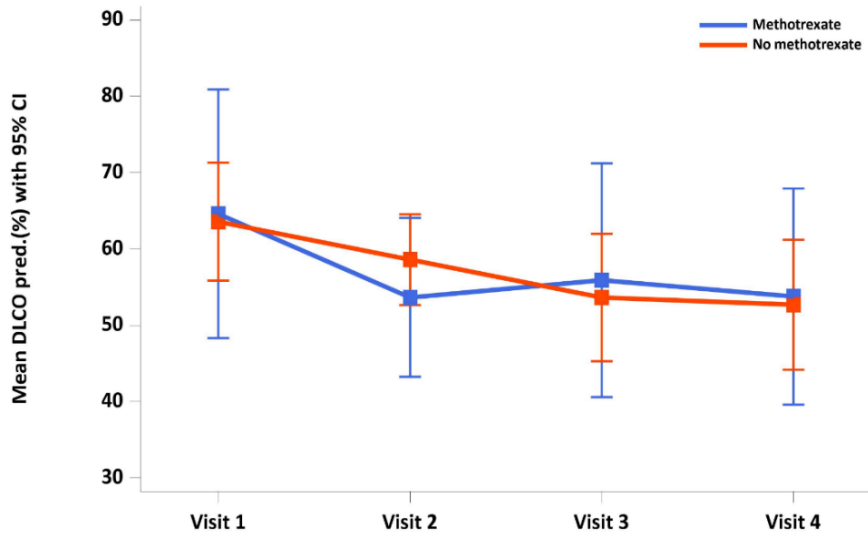

No. of Patients				
Methotrexate	12	11	10	8
No methotrexate	23	23	18	16

Table 5. Change in quantitative evaluation of chest CT scans using chest CT scoring system at three follow-up years: methotrexate versus no methotrexate

	Baseline			1-year follow-up			2-year follow-up			3-year follow-up			P **
	MTX	No MTX	P	MTX	No MTX	P	MTX	No MTX	P	MTX	No MTX	P	
Total number of patients, n	32	69		28	58		26	49		22	41		
CT abnormalities													
Pure GGO													
N (%)	10 (31.3)	24 (34.8)	0.79	8 (28.6)	21 (36.2)	0.49	7 (26.9)	19 (38.8)	0.50	7 (31.8)	15 (36.6)	0.75	0.97
Mean ± SD	0.11±0.19	0.19±0.36	0.31	0.14±0.37	0.22±0.40	0.61	0.12±0.23	0.23±0.42	0.67	0.14±0.23	0.26±0.47	0.66	1.00
Reticular opacity (RO)													
N (%)	32 (100.0)	67 (97.1)	-	28 (100.0)	57 (98.3)	-	26 (100.0)	48 (98.0)	-	22 (100.0)	40 (97.6)	-	
Mean ± SD	0.95±0.47	0.87±0.44	0.50	1.07±0.64	0.93±0.48	0.18	1.05±0.53	0.96±0.51	0.12	0.98±0.52	0.96±0.52	0.10	0.75
Traction bronchiectasis/bronchiolectasis (TB)													
N (%)	27 (84.4)	59 (85.5)	0.84	25 (89.3)	51 (87.9)	0.82	24 (92.3)	44 (89.8)	0.90	21 (95.5)	36 (87.8)	0.67	0.96
Mean ± SD	0.61±0.48	0.70±0.53	0.47	0.65±0.53	0.71±0.52	0.55	0.75±0.57	0.76±0.50	0.93	0.80±0.59	0.78±0.55	0.79	0.79
Honeycombing (HC)													
N (%)	16 (50.0)	45 (65.2)	0.23	14 (50.0)	38 (65.5)	0.37	16 (61.5)	36 (73.5)	0.39	14 (63.6)	29 (70.7)	0.50	1.00
Mean ± SD	0.23±0.33	0.40±0.49	0.11	0.27±0.42	0.41±0.51	0.24	0.37±0.46	0.47±0.52	0.50	0.38±0.50	0.49±0.57	0.69	0.91
Emphysema													
N (%)	6 (18.8)	12 (17.4)	0.97	6 (21.4)	8 (13.8)	0.41	4 (15.4)	7 (14.3)	0.83	3 (13.6)	6 (14.6)	0.92	0.90
Mean ± SD	0.07±0.21	0.12±0.36	0.51	0.07±0.20	0.11±0.38	0.63	0.06±0.21	0.13±0.41	0.57	0.06±0.22	0.12±0.41	0.54	0.04
Fibrosis A (any RO and TB)													
N (%)	27 (84.4)	59 (85.5)	0.84	25 (89.3)	51 (87.9)	0.82	24 (92.3)	44 (89.8)	0.90	21 (95.5)	36 (87.8)	0.67	0.96
Mean ± SD	1.70±0.78	1.79±0.78	0.69	1.82±0.94	1.82±0.86	0.99	1.87±0.99	1.89±0.82	0.66	1.85±1.02	1.95±0.86	0.48	0.97

Fibrosis B (fibrosis A or HC)													
N (%)	27 (84.4)	60 (87.0)	0.74	25 (89.3)	52 (89.7)	0.95	24 (92.3)	45 (91.8)	0.94	21 (95.5)	37 (90.2)	0.79	0.98
Mean ± SD	1.98±1.04	2.25±1.16	0.35	2.13±1.25	2.28±1.26	0.63	2.26±1.34	2.41±1.18	0.98	2.25±1.40	2.50±1.31	0.76	1.00
Extent													
1. < or = 10%			0.88			0.81			0.85			0.88	0.96
N (%)	20 (62.5)	42 (60.9)		17 (60.7)	35 (60.3)		13 (50.0)	24 (49.0)		11 (50.0)	19 (46.3)		
2. >10%, <30%													
N (%)	6 (18.8)	14 (20.3)		3 (10.7)	11 (19.0)		5 (19.2)	9 (18.4)		6 (27.3)	8 (19.5)		
3. >or = 30%													
N (%)	6 (18.8)	13 (18.8)		8 (28.6)	12 (20.7)		8 (30.8)	16 (32.7)		5 (22.7)	14 (34.1)		
CT abnormalities + extent													
Among patients with extent >10%													
N (%)	12 (37.5)	27 (39.1)		11 (39.3)	23 (39.7)		13 (50.0)	25 (51.0)		11 (50.0)	22 (53.7)		
Fibrosis A† (any RO AND TB)													
N (%)	11 (91.7)	27 (100.0)	-	10 (90.9)	23 (100.0)	-	12 (92.3)	25 (100.0)	-	11 (100.0)	22 (100.0)	-	
Mean ± SD	2.43±0.52	2.38±0.49	1.00	2.80±0.51	2.50±0.65	0.30	2.57±0.87	2.46±0.41	0.13	2.52±0.94	2.53±0.38	0.15	0.82
Fibrosis B‡ (fibrosis B or HC)													
N (%)	11 (91.7)	27 (100.0)	-	10 (90.9)	23 (100.0)	-	12 (92.3)	25 (100.0)	-	11 (100.0)	22 (100.0)	-	
Mean ± SD	2.95±0.78	3.13±0.97	0.65	3.40±0.83	3.25±1.13	0.73	3.21±1.18	3.18±0.81	0.37	3.18±1.31	3.31±0.92	0.37	0.91
Among patients with extent >or=30%													
N (%)	6 (18.8)	13 (18.8)		8 (28.6)	12 (20.7)		8 (30.8)	16 (32.7)		5 (22.7)	14 (34.1)		
Fibrosis A† (any RO and TB)													
N (%)	5 (83.3)	13 (100.0)		7 (87.5)	12 (100.0)		7 (87.5)	16 (100.0)		5 (100.0)	14 (100.0)		
Mean ± SD	2.63±0.32	2.51±0.61	0.79	3.05±0.38	2.79±0.78	0.08	3.07±0.42	2.63±0.36	0.04	**3.27±0.38**	**2.70±0.29**	**0.02***	0.65
Fibrosis B‡ (fibrosis A OR HC)													
N (%)	5 (83.3)	13 (100.0)		7 (87.5)	12 (100.0)		7 (87.5)	16 (100.0)		5 (100.0)	14 (100.0)		

	Mean ± SD	3.30±0.79	3.50±1.18	0.72	3.79±0.65	3.74±1.32	0.48	3.98±0.67	3.48±0.83	0.23	4.37±0.58	3.68±0.90	0.15	0.64

* P<0.05 compared between methotrexate treatment group and no methotrexate treatment group

**P-value was calculated by linear mixed-effects ordinal or binary logistic regression with random intercept model for repeated measures analysis to show the interaction effect between visit and group

†Fibrosis A was defined as the state of >0 reticular opacity scores with >0 traction bronchiectasis/bronchiolectasis scores.

‡Fibrosis B was defined as the state of fibrosis A with/without >0 honeycombing scores.

Figure 4. Change in chest CT scores of patients with lung involvement ≥30%: methotrexate versus no methotrexate: (A) pure round glass opacity, (B) reticular opacity, (C) traction bronchiectasis/bronchiolectasis, (D) honeycombing.

A.

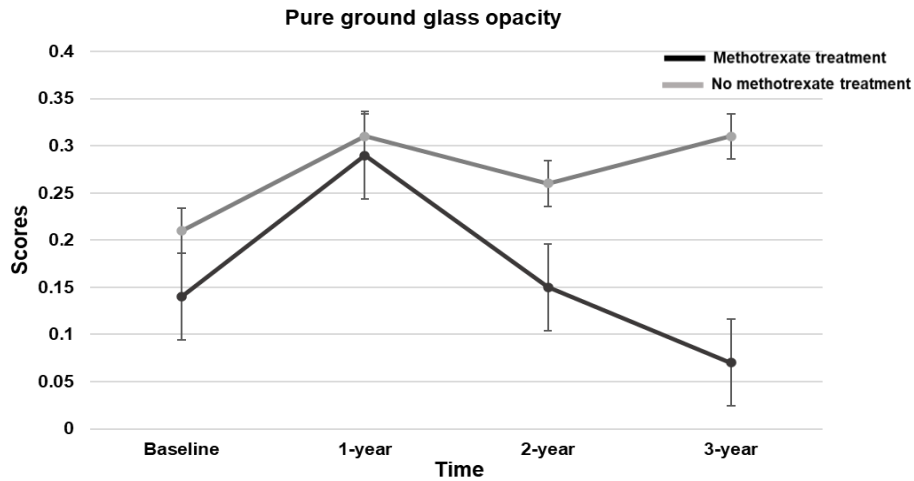

B.

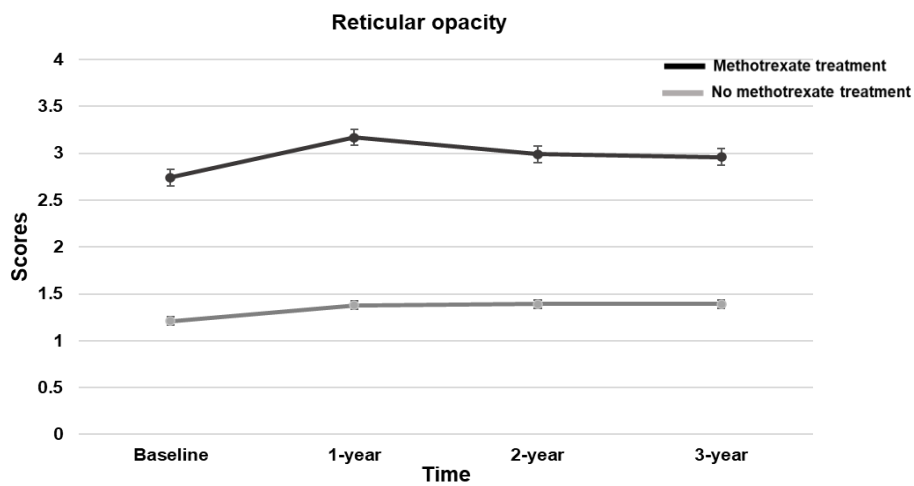

C.

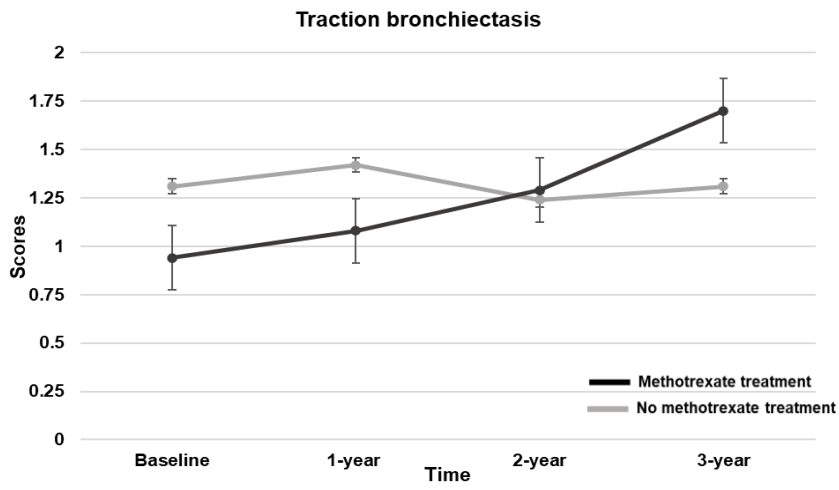
Traction bronchiectasis
2
1.75
1.5
1.25
1
0.75
0.5
0.25
0
Scores
Methotrexate treatment
No methotrexate treatment
Baseline
1-year
2-year
3-year
Time

D.

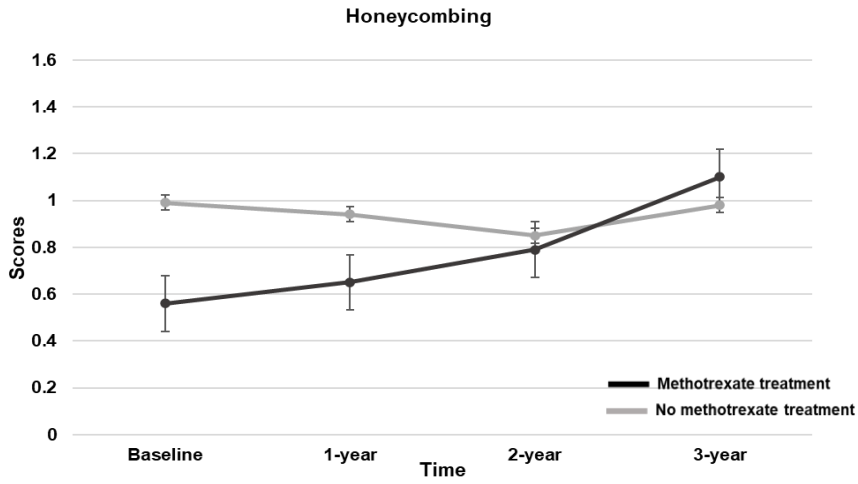
Honeycombing
1.6
1.4
1.2
1
0.8
0.6
0.4
0.2
0
Scores
Methotrexate treatment
No methotrexate treatment
Baseline
1-year
2-year
3-year
Time

Part II. Transcriptome analysis to explore the effect of disease-modifying antirheumatic drugs on the lung of rheumatoid arthritis-associated lung disease using an animal model

Introduction

The most widely used animal model for pulmonary fibrosis is the bleomycin-induced lung fibrosis model.[21, 40] However, this model does not develop arthritis. There are several animal models for arthritis, but only three develop lung disease[21]: the tumor necrosis factor-transgenic model, the adjuvant arthritis model, and the SKG mouse. The SKG mice are of the BABL/c mouse background strain with a spontaneous point mutation of the gene-encoding SH2 domain of ZAP-70, a critical signal transduction molecule in T cells, as reported by Sakaguchi et al. in 2003.[41] The altered ZAP-70 molecule attenuates the downstream signal transduction of T cells for self-peptide, increases their avidity reactive to self-peptide, escapes from the thymus, and enters the peripheral circulation. As in humans, these pathogenic T cells need environmental stimulation to activate immune cell diseases. Patients with RA have autoimmune T cells, but they do not develop arthritis in specific-pathogen free (SPF) environment without a trigger, such as zymosan (a crude yeast cell wall extract), which activates immune cells via its main component, β-glucans.[42] The mice then develop various autoimmune disease features, including synovitis, pneumonitis, vasculitis, subcutaneous nodules, and autoantibodies such as rheumatoid factor. Therefore, they are suitable for a murine arthritis model with extra-articular manifestation.

Recent advances in scientific technology, especially omics techniques, have significantly expanded understanding of biological processes. Proteomics, the most functional field of omics, is limited due to limited probes or antibodies. Although whole-genome DNA sequencing provides massive amounts of biological data, it cannot assess which genes are turn-on or turn-off. Therefore, transcriptomes that encompass total messenger RNA (mRNA)-delegating functional genes have been widely adopted for research. Microarrays, the oldest method for analyzing transcriptomes, have several limitations; they explore a limited number of mRNAs due to their defined sequence and restricted spatial plate. It is challenging to quantify mRNAs because of ambiguous gene activity due to relative fluorescence intensity estimation. Sequencing of RNA provides whole-RNA data using next-generation sequencing (NGS) technology to handle massive data processing. While bulk RNA sequencing lumps the signal changes of entire tissues, single-cell RNA sequencing dissociates signal changes of each cell that provide more sophisticated pathologic changes. In single-cell RNA sequencing, mechanical disaggregation or enzymatic dissociation with collagenase and DNase is required to separate each viable cell. During these procedures, a part of genes other than immune cells can be underrepresented during dissociation to a single cell; those procedures are highly tissue specific and are determined empirically.[43-45] To acquire viable single cells, samples should be fresh and unfrozen; these are not readily available, especially in the case of rare samples.

Single-nucleus RNA sequencing, which analyzes RNA of a nucleus extracted from a single cell, has the advantage of being able to use frozen tissue; however, information in the cytoplasm cannot be obtained.[43-45] Of note, current dissociating

single-cell protocols may be challenging to use in separation of non-immune cell populations, such as airway/alveolar epithelial cells, and may underestimate those cell populations.

In the current study, we aimed to analyze and compare the effect of methotrexate and TNFα inhibitor on lung tissue of SKG mice using single-nucleus RNA sequencing.

Materials and methods

Mice

SKG mice (CLEA Japan, Inc.) at age 7-12 weeks were used. All mice were kept in specific pathogen-free conditions within the Gyerim Experimental Animal Resource (GEAR) Center. All experiments were approved by the Institutional Animal Care and Use Committee of the Soonchunhyang University Research Institute (IACUC No: SCH20-0037, SCH19-0061, SCH21-0045).

Induction of arthritis and pneumonitis in murine disease model and treatment

At age eight to ten weeks, male SKG mice received a single intraperitoneal zymosan injection (7.5 mg per 20g; MilliporeSigma, St. Louis, MO, USA) to induce arthritis and pneumonitis. We then gave them twice-weekly intraperitoneal injections of PBS, methotrexate (7.5 mg/kg; MilliporeSigma), or TNFα inhibitor (100 μg/kg; R&D Systems, Inc., Minneapolis, MN, USA). The treatment schedule is summarized in Figure 5.

Histology of the lung

The left lung of each injected mouse was inflated with 4% paraformaldehyde, embedded in paraffin, and sectioned. The sections were stained with hematoxylin and eosin. The right lung was resected, snap-frozen in liquid nitrogen, and stored at -80℃.

Immunofluorescence staining of lung

Each paraffin-embedded lung section was sliced into 5μm sections and deparaffinated. Briefly, each slide was rinsed twice with PBS for 5-10 minutes at room temperature, incubated with preheated heat-induced epitope retrieval (HIER) buffer for 15-30 minutes at 95-99 ℃, then treated with cold PBS for 20 minutes on ice. For membrane permeabilization, the samples were treated with PBST (PBS with 0.1% Triton X100) for 10 minutes at room temperature, then incubated with 2-5% serum in PBST for 30 minutes to block nonspecific antigen-antibody reaction. Next, the samples were incubated with primary antibody overnight at 4℃, followed by incubation with secondary antibody. Primary antibody targeting α-SMA (catalog number sc-53142) and isolectin B4 (catalog number L2895) were purchased from Santa Cruz Biotechnology, Inc. (Dallas, TX, USA), and MilliporeSigma, respectively.

Assessment of joint

Arthritis scores were assessed weekly by visual inspection and scored as follows: 0 (no evidence of erythema or swelling); 1 (erythema and mild swelling confined to the tarsals or ankle joint); 2 (erythema and mild swelling extending from the ankle to the tarsals); 3 (erythema and moderate swelling extending from the ankle to metatarsal joints); 4 (erythema and severe swelling encompassing the ankle, foot, and digits, or ankylosis of the limb). The mean scores of both forepaws and hindpaws were calculated.

Single-nucleus preparation from frozen mouse lung

Nuclei were prepared from frozen lung tissue under ribonuclease-free conditions by a method adapted from an existing protocol.[46] Briefly, samples were cut into ~7mm pieces, injected via 26 gauge needle with 1 ml of ice-cold Nuclei EZ Lysis buffer (NUC101; MilliporeSigma) supplemented with a protease (589279100; Hoffmann-La Roche Ltd, Basel, Switzerland) and ribonuclease (RNAse, N2615; Promega Corp., Madison, WI, USA) inhibitor (250 units/ml RNasin® Plus N2615; Promega Corp., Madison, WI, USA), minced to 1-2 mm pieces with scissors in a weigh boat with 1 ml additional supplemented lysis buffer, then transferred to a gentleMACS™ C tube (Miltenyi Biotec, Bergisch Gladbach, Germany). The gentleMACS *lung1* and *lung 2* programs were run in sequence, and the latter stopped after 20 seconds. The foam was spun down for 10 seconds using a short spin. The suspension was passed through a 40-µm cell strainer and washed with 4°C cold PBS with 1% bovine serum albumin (BSA). Nuclei were pelleted at 500xg; resuspended in 1X PBS with 1% BSA and 0.5 units/µl RNasin Plus; counted by hemocytometer and diluted to 1,000 nuclei/µl. For 10X Chromium, 10,000 nuclei were loaded per lane. The 10x Chromium libraries were prepared according to the manufacturer's protocol (10x Genomics, Pleasanton, CA, USA) using 3′ V3.1 kits and were submitted for sequencing through the Geninus Inc. laboratory, Seoul, Korea, on a NovaSeq S1 flow cell to a depth of 50,000 reads/cell.

Library preparation and sequencing

Raw sequencing data were processed using the zUMIs pipeline, removing low-quality barcodes and then mapping the remaining barcodes to the mouse genome (mm10) using Cell Ranger v4 (10x Genomics). Expression matrixes containing

intronic, exonic, and nitronic+exonic reads were generated for single-nucleus RNA sequencing (snRNA seq) data (Figure 2).

After that, we used additional filtering using Seurat 4 with R 4.0.1 (Satija Lab, New York, NY, USA). We filter cells using UMI counts, Expressed gene counts, and mitochondria percentage. After filtering, we normalize data and find variable features using VST technique (n=2,000) and Scale data in each dataset. Finally, we integrated data using run Harmony command in Harmony R packages to mitigate the batch effect since we conducted experiment by treatment group. [47]

For clustering, Next, we calculated Uniform Manifold Approximation and Projection (UMAP) using harmony value as reductions. and primary cell annotation was tagged using RCA and SCSA. Secondary cell annotation was done manually, based on primary cell annotations.

Results

Establishment of animal model for RA-ILD using SKG mice

To determine the zymosan A dose, we tried injections of zymosan A 5 mg/20g or 7.5 mg/20g in SKG male mice. As a result, 7.5 mg/20g zymosan A administration showed more severe pneumonitis. Therefore, we decided to use zymosan 7.5 mg/20g.

Arthritis mitigation in SKG mice with zymosan A and methotrexate or TNFα inhibitor treatment

Next, to investigate the effect of DMARDs on the lung of the RA-ILD animal model, we gave PBS, methotrexate, or TNFα inhibitor treatment for 12 weeks intraperitoneally to SKG mice that had been injected with zymosan A. As expected, no swelling was observed in mice not injected with zymosan A, and severe swelling was observed in mice with zymosan A and PBS treatment. Joint swelling was mitigated with methotrexate or TNFα inhibitor treatment. Most of the mice with zymosan A and methotrexate treatment showed minimal joint swelling (Figure 7).

Pneumonitis was the most profound in mice with zymosan A and methotrexate treatment

The lung histology with hematoxylin and eosin staining is shown in Figure 8 and 9. Macroscopically, pneumonitis was most evident in SKG mice with zymosan A and methotrexate treatment; multiple inflammatory cell aggregations were observed (Figure 8). In mice with zymosan A and TNFα inhibitor, there were a few perivascular inflammatory cell aggregations as in the mice with zymosan A and PBS, compared with the mice without zymosan A (Figure 9). Immunofluorescent staining

revealed many immune cells and myofibroblast cells at the foci. The ciliated cells and club cells were comparable among the four treatment groups. Representative images of tissue are shown in Figure 10.

The single-nucleus cell analysis of lung tissue revealed the different proportions according to treatment

A total of 59,860 nuclei were obtained from sixteen mice, four mice from each of the four groups. Unsupervised clustering of single-nucleus data resulted in 35 clusters after dimensional reduction using Seurat version 3.2.2 (Satija Lab, New York, NY, USA). We classified each cell type using previous reports on the single-nucleus cells of mouse lungs (Figure 11).[46] Classification of cell types and signature genes of each cell group are denoted in Figure 11 and 12A.

The most frequently observed cell type was immune cells, followed by epithelial cells across the treatment groups, and the most observed cell was the type 2 alveolar cell (Figure 12B).

Immune cell proportion dynamics associated with zymosan A injection were further accentuated by methotrexate, but not by TNFα inhibitor

Immune cells showed dynamic changes in cell type according to group (Figure 12C). In the mice without zymosan A injection, alveolar macrophage was the most prevalent cell, followed by T and B cells. This proportion was altered by zymosan A treatment, after which T cells were the most frequently observed, followed by alveolar macrophage, B cells, and polymorphonuclear cells. Methotrexate treatment of mice with zymosan A injection showed greater accentuation of these cell type

proportions; T cells, B cells, and polymorphonuclear cells increased relative to alveolar macrophages. Interestingly, TNFα inhibitor treatment of mice with zymosan A attenuated these cell proportions and instead reverted to the cell proportion of those mice without zymosan A; alveolar macrophage was the most frequently observed cell type in this group. Instead of T cells, B cells were the second most frequent cells in mice with zymosan A and TNFα inhibitor treatment.

Next, we analyzed transcriptome changes in immune cells by treatment. Most of the up-regulated genes compared with mice without zymosan A injection originated from alveolar macrophage cells in all three treatment groups (Figure 13).

Methotrexate treatment accentuated pathological transcriptome signature of alveolar macrophage cells and enriched interferon response signaling

When zymosan A was injected, 478 genes were up-regulated and 541 genes were down-regulated in alveolar macrophage cells (Figure 13A). Those transcriptomes were subclustered using up- or down-regulated genes in methotrexate-treated and TNFα inhibitor-treated mice with zymosan A injection, compared with mice without zymosan A injection. Six clusters of genes were created. Clusters 1, 2, and 3 were up-regulated whereas clusters 4, 5, and 6 were down-regulated. Among up-regulated transcriptomes, cluster 1 were genes that were commonly down-regulated by methotrexate or TNFα inhibitor treatment. Cluster 3 genes were down-regulated with methotrexate treatment whereas cluster 5 was up-regulated. Cluster 4 genes were up-regulated with TNFα inhibitor treatment.

Interestingly, in cluster 2, which was up-regulated, genes were further up-regulated by methotrexate treatment while TNFα inhibitor down-regulated them. Cluster 2 was

enriched with interferon gamma (IFNγ) response, mTORC1 protein complex signaling, and TNFα signaling via NF-kB pathway signals. Transcriptomes in cluster 6, down-regulated by zymosan A injection, were further down-regulated by methotrexate treatment.

Next, we compared changes of the transcriptomes by methotrexate or TNFα inhibitor treatment with PBS- treated mice (Figure 13B). Notably, transcriptomes up- or down-regulated by anti-TNFα inhibitor treatment did not have any significantly enriched signaling pathway while those up-regulated by methotrexate treatment revealed greatly enriched IFNα and IFNγ response.

Interferon signaling was enriched in T cells by methotrexate treatment compared with PBS treatment in mice with zymosan A injection

In T cells, zymosan A injection up-regulated only 19 genes, which were commonly down-regulated by methotrexate or TNFα inhibitor treatment (Figure 14A). A total of 473 genes were down-regulated by zymosan A injection. In subclustering using up- or down-regulated genes in methotrexate-treated and TNFα inhibitor-treated mice, four clusters were noted. Clusters 2 and 3, down-regulated by zymosan A injection, consisted of genes further down-regulated or up-regulated, respectively, by methotrexate and TNFα inhibitor. Genes of cluster 4 were up-regulated by TNFα inhibitor treatment.

Comparing changes in genes by methotrexate or TNFα inhibitor treatment, methotrexate resulted in 53 genes up-regulated compared with 133 genes down-regulated. Interestingly, however, those fewer numbers of genes up-regulated by methotrexate were strongly enriched with IFNα and IFNγ responses (Figure 14B).

Increased proportion of fibroblast subclusters poorly enriched with response to nintedanib in PBS-treated and methotrexate-treated mice

Fibroblasts were subclustered into seven clusters (Figure 15). Clusters 0, 1, 2, 3, and 4 were Pdgfra^{lo}lipofibroblast, Pdgf^{lo}Fgfr^{lo}fibroblast, Pdgfrb^{hi}fibroblast, matrix fibroblast, and myofibroblast, respectively. In mice without the zymosan A injection, cluster 3 was dominant. With the injection, clusters 0, 1, and 2 were increased while a very low proportion of cluster 3 was observed. After methotrexate treatment, clusters 2 and 3 increased, while TNFα inhibitor treatment widely altered those compositions to increase cluster 0.

In PBS-treated and methotrexate-treated mice, cluster 1 was the dominant cluster in those groups poorly enriched with nintedanib perturbated-response genes (Figure 16). Of note, with TNFα inhibitor treatment, the proportion of cluster 1 was lower while the ratio of cluster 0 was higher.

Alveolar cell subcluster analysis showed a distinct cell population in the methotrexate treatment group

Alveolar cells were further subclustered into six clusters (Figure 17A). Cluster 2 highly expressed AT1 marker genes, including Rkn2, Hopx, and Cav1. In mice without zymosan A injection, cluster 0 predominated relative to cluster 1 (Figure 17B). This proportion was inverted in mice with the injection, where cluster 1 predominated. TNFα inhibitor treatment reversed the proportion, with cluster 0 predominating in this group. On the other hand, methotrexate treatment further

accentuated the predominance of cluster 1 over cluster 0. Interestingly, a distinct cluster 3 was observed after methotrexate treatment.

A distinctive subpopulation of alveolar cells in the methotrexate treatment group showed IL-1β/TNF perturbated-response signatures and reduced regeneration capacity

The Library of Integrated Network-Based Cellular Signatures (LINCS) is a Common Fund program of the U.S. National Institutes of Health that catalogs how human cells globally respond to chemicals, genetics, and disease perturbations. The LINCS L1000 project is a collection of transcriptome assay measures 978 landmark transcriptomes from perturbated cells with Luminex- based detection on 384-well plates. The unmeasured transcriptome can be computationally inferred from these landmark genes using a trained algorithm. Gene set enrichment analysis (GSEA) was conducted using cytokine-responsive gene sets originating from each cytokine-treated cell (LINCS 1000 ligand perturbation analysis). A distinctive alveolar epithelial cell cluster of the methotrexate treatment group showed IL-1, TNF, IFNα, and IFNγ perturbation-response signatures.

The gene BMI1 is essential for self-renewal of stem cells in many tissues, such as lung epithelial stem cells. BMI1 knockout mice exhibit many derepressed imprinted genes and fail to self-renew their lung cells.[48] Enrichment analysis was performed using BMI1 knockout mice genes, and the BMI1 knockout mice gene module was significantly enriched in cluster 3 as well as in cluster 2, alveolar cell type 1.

Discussion

Interstitial lung disease associated with RA is a systemic inflammatory disease that produces arthritis along with pneumonitis. The bleomycin-induced pneumonitis model is mainly used as the animal model of pulmonary fibrosis or lung inflammation, but signs of systemic inflammation such as arthritis are rarely observed in this model. Mice of the SKG strain are an animal model in which symptoms such as arthritis and pneumonia occur due to environmental triggering such as β-glucan in the genetic background of Zap-70 point-mutation; this is very similar to the onset of autoimmune diseases in humans. As if reflecting this context, immune cell populations showed the most dynamic proportion change by treatment. Among them, alveolar macrophage showed the largest number of genes up-regulated by zymosan A injection.

Alveolar macrophages, abundant in the lung, are a specialized lung macrophage population. They mainly present in the alveoli and play a role not only in first-line defense but also in maintaining lung homeostasis, including removal of surfactants.[49-51] Alveolar macrophages play a role as inflammatory macrophages that secrete IFNγ, TNFα, and Interleukin-1-beta (IL-1β) in the inflammatory milieu, or as alternative activated macrophages that contribute to fibrotic pathology in the process of inflammation resolution. In addition, besides tissue-resident alveolar macrophages of embryonic origin, they can be replenished by recruiting bone marrow-derived macrophages in situations such as lung insult.[49] A profound modification within pulmonary macrophage populations has been reported during the course of IPF; highly proliferative SPP1 ^{hi} macrophages were observed, constituting a new target to deplete profibrotic macrophages in IPF lungs.[52, 53]

In the current study, the protein interaction network showed STAT1 as a network hub in PBS- treated mice, and two additional major hubs—hypoxia inducible factor 1A (HIF1A) and interferon regulatory factor 1 (IRF1)—were observed in methotrexate-treated mice, while there was no network hub in those treated with the TNFα inhibitor. Those three hubs are the same hubs reported in previous research on microarray analysis of fungal infections in mice.[54] In that study, STAT1, HIF1A, and IRF1 were expressed more strongly in an infection-resistant mouse strain than in an infection-susceptible strain. Along with an increase in type II interferon, resistance to fungal pathogen was associated with activation of NF-kB and subsequent HIF1A due to an increase in TNFα. Considering that zymosan A is a fungal component extract, the analysis results of alveolar macrophage in the current study seem to reflect innate immunity rather than adaptive immunity—the main mechanism of autoimmune disease. Indeed, in the present study, the change in the transcriptome of T cells was not significant compared to that of alveolar macrophages. Considering the previous studies that found that pneumonitis was followed by arthritis and that pneumonitis occurs after 12 weeks or as late as 24 weeks,[41, 42] it is speculated that different results might be seen with a more extended observation period after zymosan A injection. Nevertheless, in spite of the aforementioned findings on immune cells (a longer observation period may have been required to show autoimmune features), the methotrexate-treated group showed pathologically evident inflammation. This suggests that cell types other than immune cells may play a greater role in the pathology shown in current disease animal model studies.

Single-cell RNA sequencing has the advantage of drawing a detailed picture of the onset and course of a disease by detecting minute changes at the cellular level. However, there are lost or damaged cells in single-cell RNA sequencing during single-cell separation. Accordingly, morphologically larger and irregular non-immune cells can be underestimated in comparison to immune cells. Non-immune cells such as epithelial cells and fibroblasts occupy a significant proportion of lung tissue, and these cells are involved in pathogenesis. These non-immune cells tend to disappear in single-cell RNA sequencing, but they tend to be more accurately detected in snRNA seq.[46]

In the present study therefore, we focused on alveolar cells to investigate the drug's effect on the lungs. The study revealed that transcriptome change existed before evident histological change developed in the lungs of murine RA-ILD models. Methotrexate treatment heightened the effect of zymosan A on the lungs, whereas TNFα inhibitor treatment reduced it.

The lungs are vulnerable and constantly exposed to insults from the external environment, including infection. The lungs continually undergo repair and regeneration in response to such insults. Among two primary lineages in the alveolar epithelium, i.e., the alveolar type 1 (AT1) cells, and alveolar type 2 (AT2) cells, AT2 mainly play this regeneration role in the distal airway.[55] Although AT1 cells function as gas exchangers coordinated with the endothelial plexus and occupy 95% of lung surface, most AT1 cell lineage lacks regenerative or differentiation capacity. On the other hand, AT2 cells, although occupying small portions of the lung surface, have dual functions as progenitor cells for regeneration and producers of lung surfactants. In homeostatic conditions, AT2 cells are quiescent and seldom proliferate. However,

in the milieu of lung damage, they can proliferate and differentiate into AT1 cells, thereby maintaining the integrity of the alveolar epithelium cells.

Repeated epithelial injuries in the distal lung followed by abnormal wound healing response leads to IPF.[56] Histologically, hyperplasia of AT2 cells and loss of AT1 cells are observed along with the hallmark features of IPF, namely aberrant epithelial cells and mesenchymal expansion.[57] Hypertrophic and hyperplastic AT2 cells in the fibroblast foci are known to lose their renewal capacity.[58] As AT2 cells are burdened with substantial biosynthetic and metabolic work, chronic damage to AT2 cells results in disrupted proteostasis, increased autophagy/mitophagy, and shortening telomere length. In addition, dysfunctional AT2 cells lose their capacity to regenerate and stay in a transitional state. Single-cell transcriptome analysis discloses such an arrested transitional cell state between AT2-to-AT1 differentiation. In humans, those arrested cells were described as Krt5-/Krt17+ aberrant basaloid cells, while they were described as Krt8+ alveolar progenitor (ADI), damage-associated transient progenitors (DATP), pre-alveolar type 1 transitional cell-state (PATs), and Cdc42-null AT2 in mice.[59] This functional defect makes AT2 cells profibrotic, apoptotic, senescent, hyperproliferative, and inflammatory. AT2 cells are not just depleted in the fibrotic lung as collateral damage to ongoing injury: in addition, these cells have acquired a dysfunctional phenotype that places them as a central driver of fibrosis.[60] In the current study, methotrexate treatment of zymosan A-injected SKG mice showed distinct alveolar type cell clusters. Cluster 3 exhibited late type 2 alveolar cell markers, including Lcn2, Il33, and Lyz2.[61] Aged AT2 cells also showed aged AT2 cell features such as a substantial increase of the major histocompatibility complex (MHC) class I genes, including H2-K1, H2-D1, and B2m, and up-

regulation of the enzyme Acyl-CoA desaturase 1(Scd1) gene.[62] Increased expression of these genes indicates that cluster 3 AT2 cells were in senescence, a state in which differentiation functions are mitigated.[61, 63, 64] The cellular senescence feature of this cluster is further supported by the fact that significant enrichment with the Bmi1 knockout mice gene set, in which the imprinted gene is derepressed, resulted in decreased cell regenerative function.[65] With methotrexate treatment, this suggests that AT2 cells induce a state of cellular senescence in which they lose their regenerative function rather than arrest in the process of differentiation into AT1, which is very similar to the features of AT2 cells shown in IPF.

Of note, induction of lung inflammation also affects lung fibroblasts. In the current study, fibroblasts were subclustered into seven clusters. Cluster 2 and 3 fibroblasts were dominant in the methotrexate- treated mice. Unfortunately, the transcriptome of cluster 2 revealed no sign of the nintedanib-treated gene signature. Nintedanib, a tyrosine kinase inhibitor, is highlighted as a treatment for progressive fibrosing ILD, including RA-ILD.[25, 66] Although it showed successful results in retarding the annual decline of lung function, the studies were mainly targeted toward patients who already had moderate or severe fibrosis with deteriorating lung function. In the current study, considering that the lung histology of the PBS-treated mice did not show evident changes, it can be speculated that the transcriptome changes of those groups represent early changes of chronic pneumonitis. Considering those points, the study results showing that cluster 1, which was supposed to be refractory to nintedanib, was the dominant cluster in the PBS- treated mice indicates that treatment other than nintedanib may be required in the early stage of chronic lung inflammation associated with arthritis. It is noteworthy that the methotrexate-treated

mice showed evident lung inflammation and fibrosis on histology; the proportion of clusters 2 and 3 enriched with nintedanib response genes was increased to that of the PBS-treated mice.

In conclusion, the current study shows that methotrexate exacerbates lung inflammation via attenuation of the regenerative potential of type 2 alveolar cells.

Figure 5. Induction and treatment schedule for SKG mice: 8-10 weeks of aged male SKG mice received a single intraperitoneal zymosan A injection (7.5 mg/20g) or no injection. Among the injected mice, three groups were classified by type of treatment: PBS, methotrexate (7.5 mg/kg), and TNFα inhibitor (100 μg/kg) twice a week intraperitoneally.

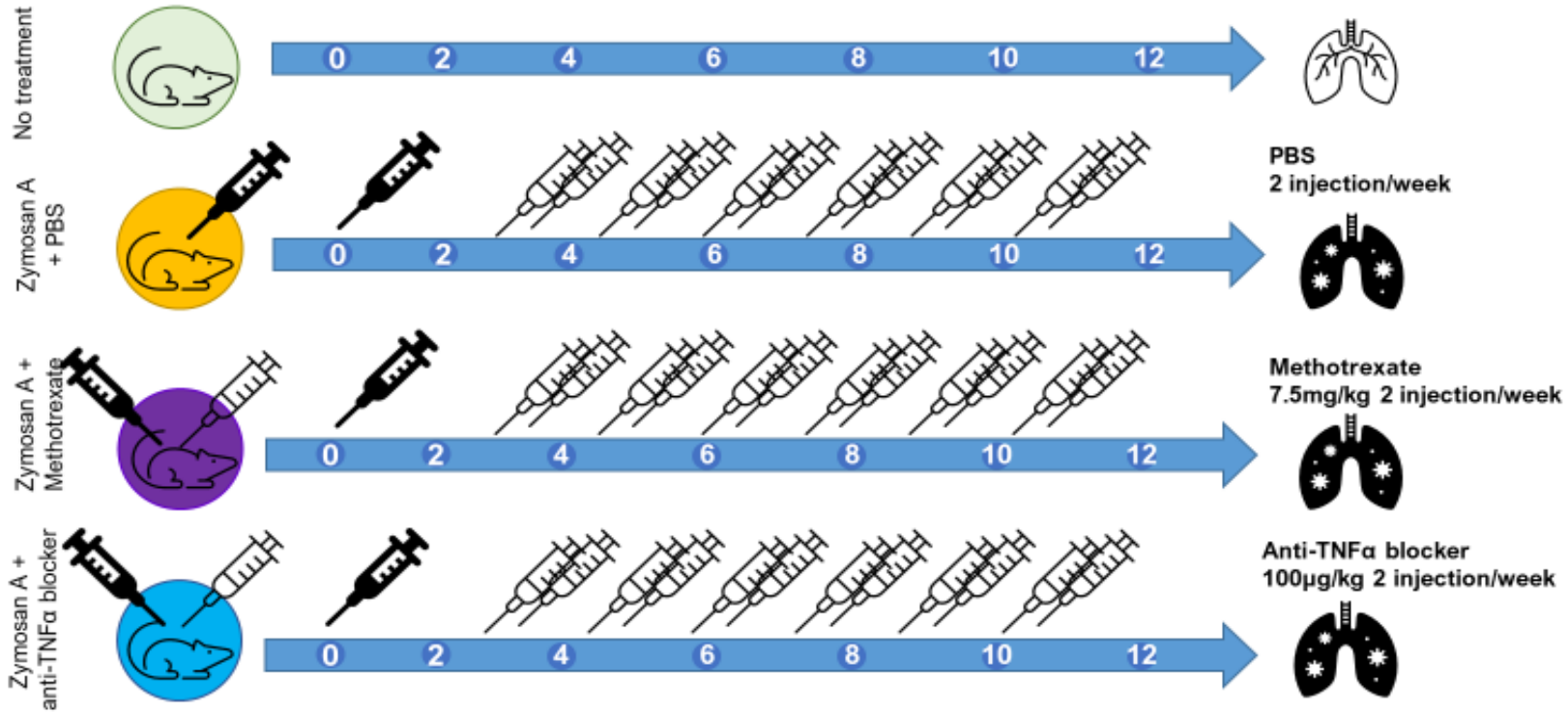

Figure 6. Workflow of (A) lung single-nucleus isolation and (B) analysis after sequencing by 10x Chromium: nuclei were extracted from the samples and libraries were constructed using 10x Chromium, and the data were processed by Seurat.

A.

B.

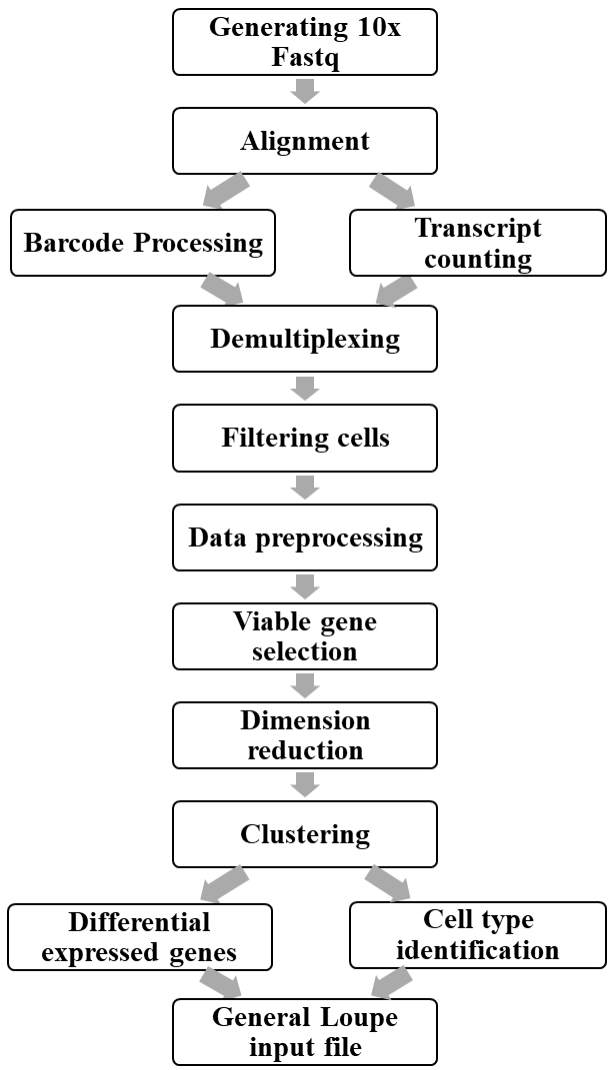

Figure 7. Change in arthritis scores of SKG mice with zymosan A injection according to treatment: (A) PBS, (B) methotrexate, (C) TNFα inhibitor.

A. PBS treated SKG mice with zymosan A injection

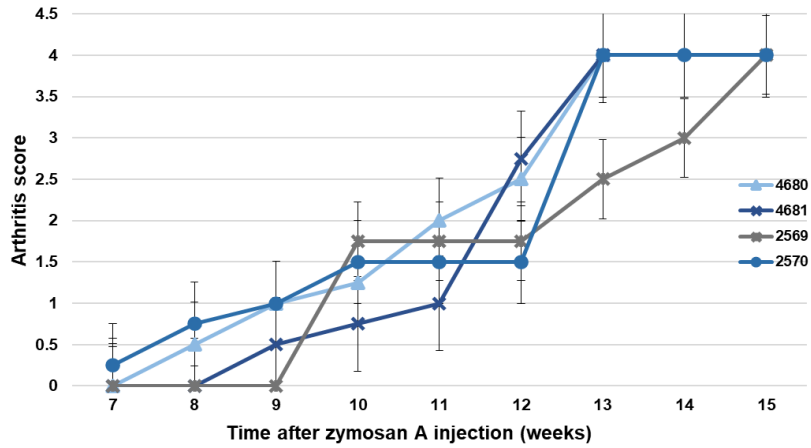

B. Methotrexate treated SKG mice with zymosan A injection

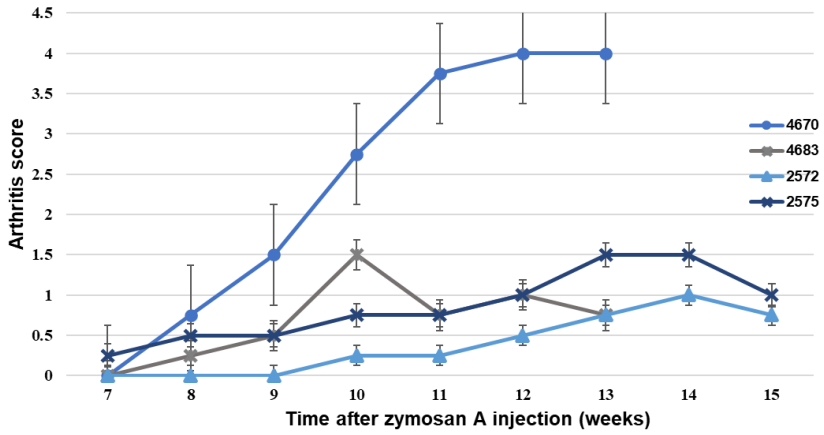

C. Anti-TNFα blocker treated SKG mice with zymosan A injection

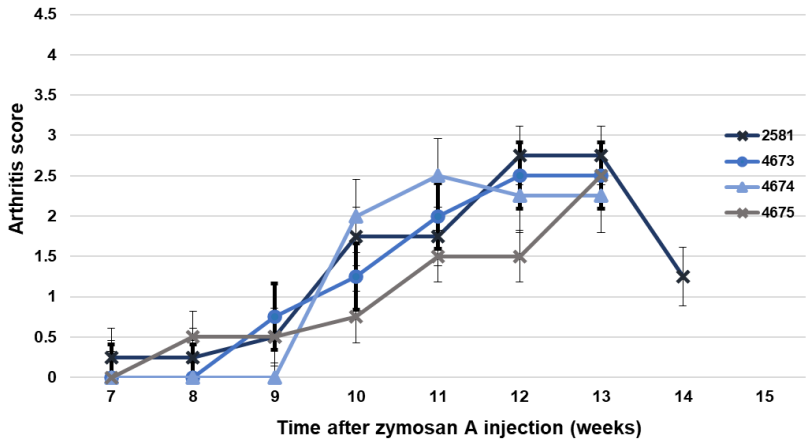

Figure 8. Gross lung tissue hematoxylin and eosin stain histology of SKG mice with zymosan A injection according to treatment: (A) PBS, (B) methotrexate, (C) TNFα inhibitor.

A. PBS treated SKG mice with zymosan A injection

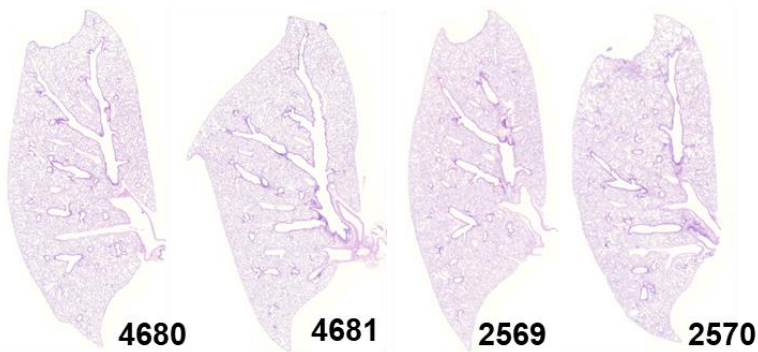

B. Methotrexate treated SKG mice with zymosan A injection

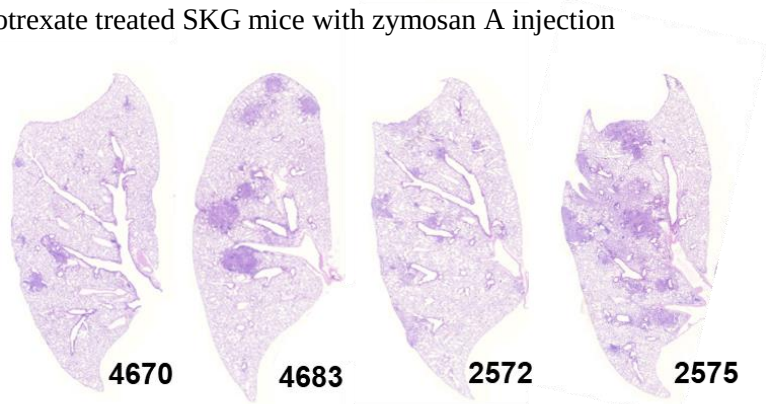

C. Anti-TNFα blocker treated SKG mice with zymosan A injection

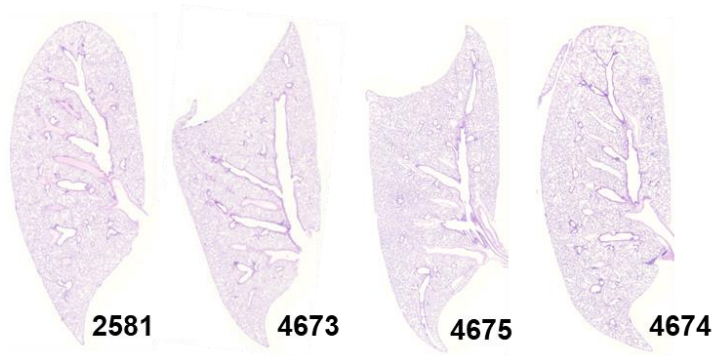

Figure 9. Representative histology with magnified peribronchovascular cell aggregation in lung of SKG mice (40X) : (A) No zymosan A injection—no cell aggregation was observed; (B)Zymosan injection, treatment with PBS—a small number of cell aggregations were observed; (C) Zymosan injection, treatment with methotrexate; (D) Zymosan injection, treatment with TNFα inhibitor. No cell aggregation was observed in mice that did not receive the injection or treatment.

A. SKG mice without zymosan A injection

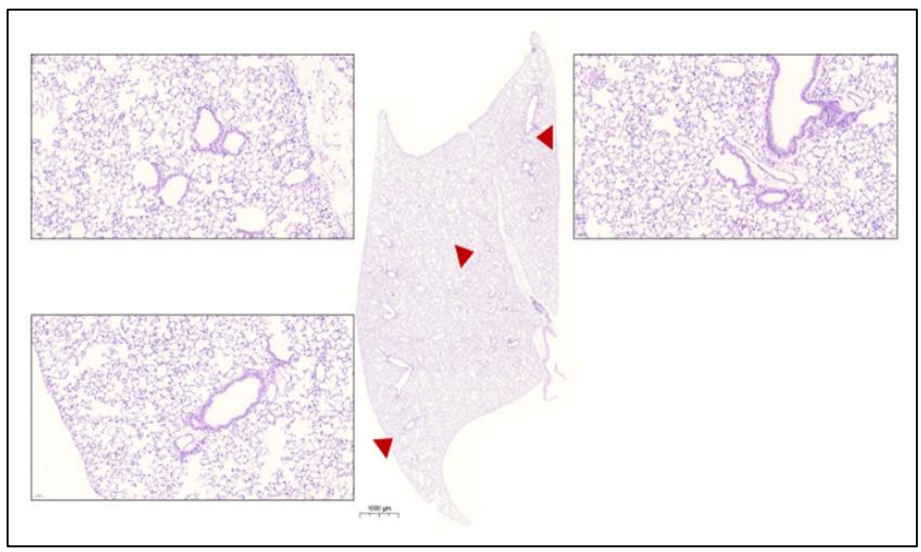

B. PBS treated SKG mice with zymosan A injection

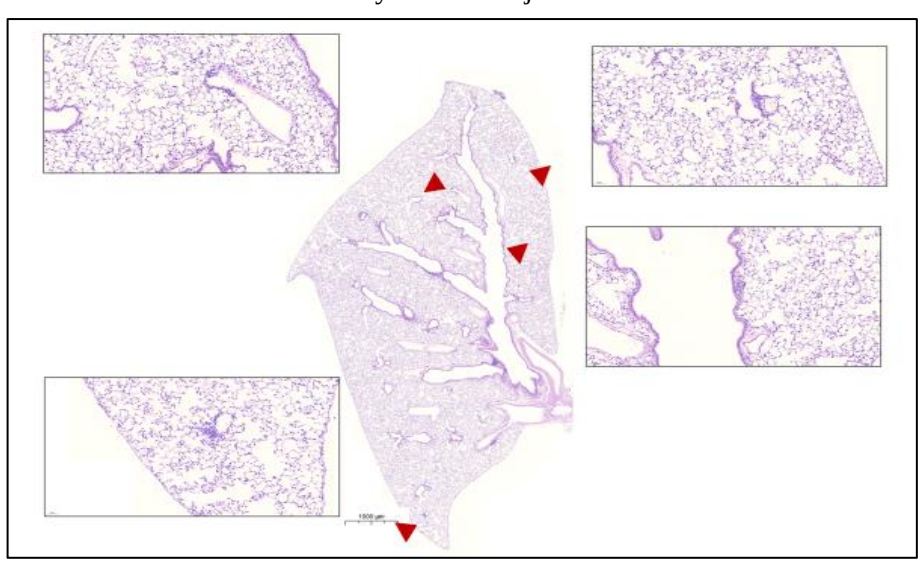

C. Methotrexate treated SKG mice with zymosan A injection

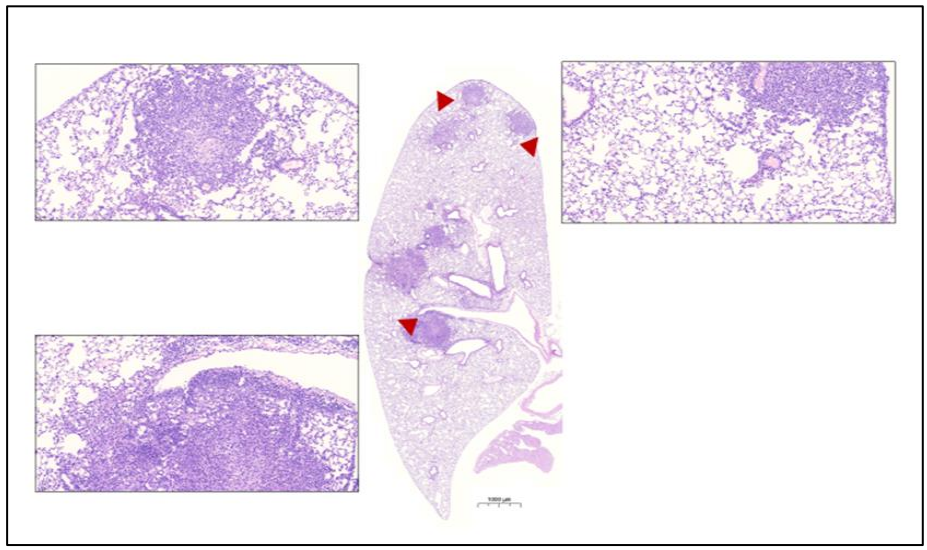

D. Anti-TNFα blocker treated SKG mice with zymosan A injection

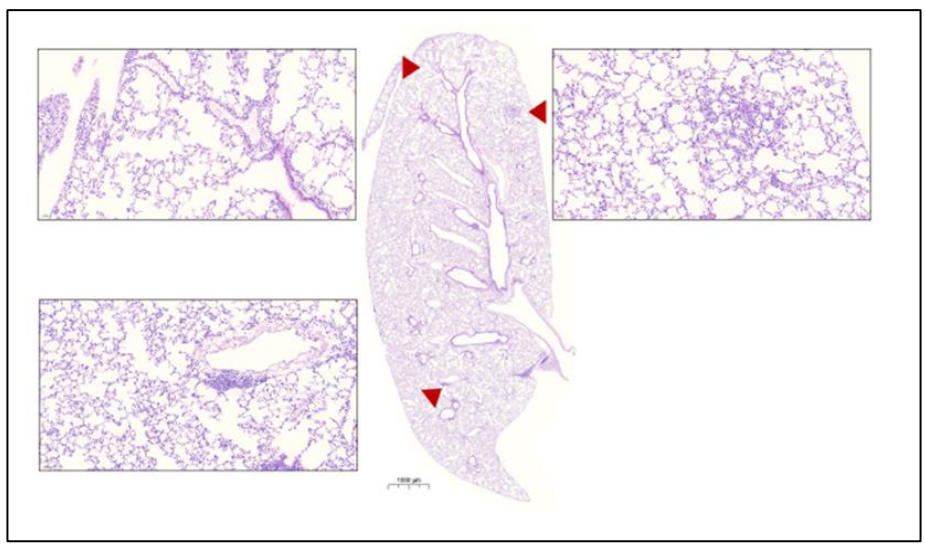

Figure 10. Immunofluorescence staining of fibroblast (α-SMA, red)/immune cells (isolectin B4, green) of SKG mice in each treatment group (left lung 40X, right lung 10X). Immune cells and fibroblast increased markedly in mice with zymosan A injection and methotrexate-treatment.

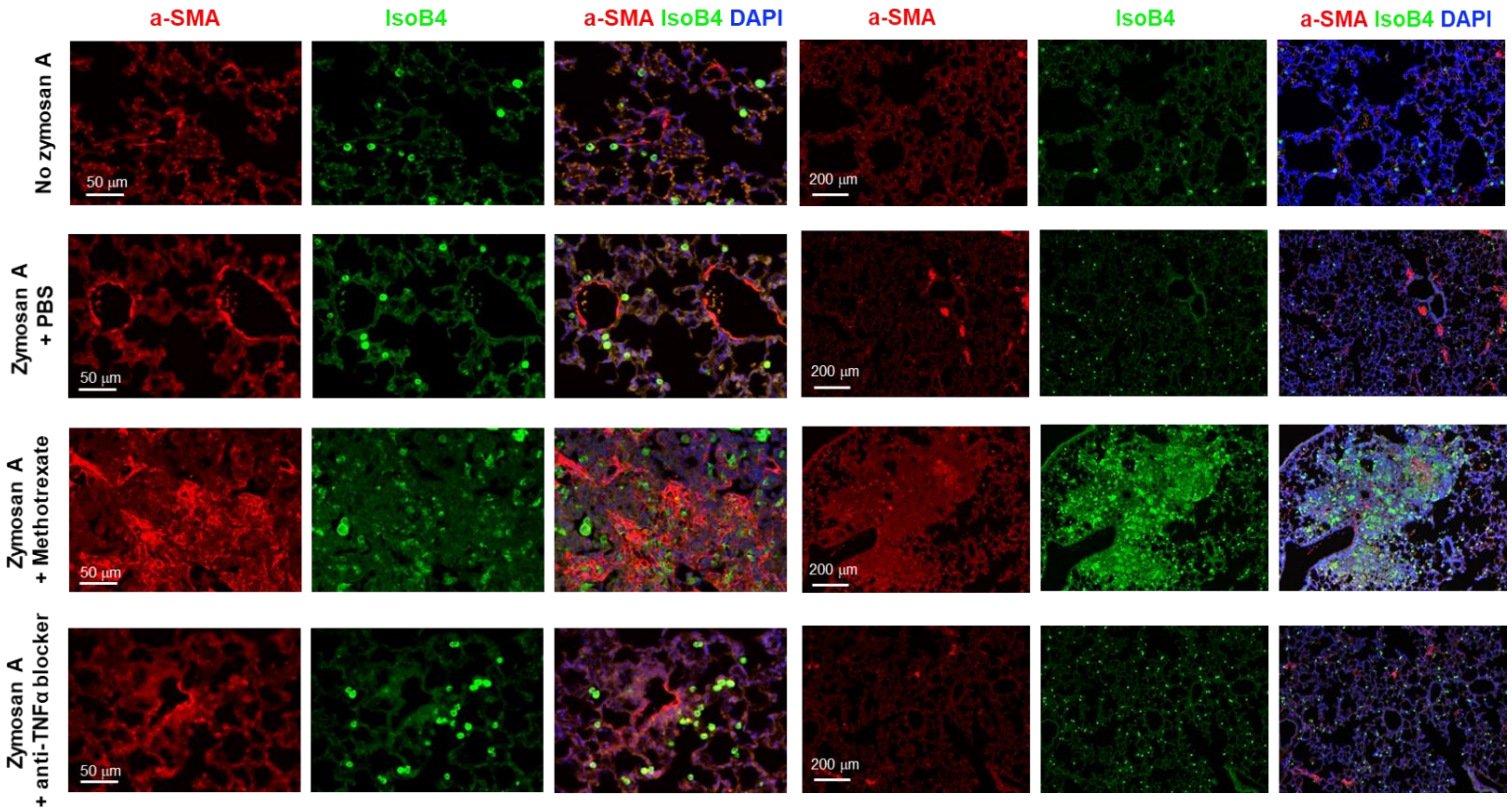

Figure 11. Integrated single-nucleus RNA analysis of SKG mice identifying diverse lung cell population: (A) UMAP plot of 59,860 nuclei from merged snRNA seq data (combined from all 16 mice), identifying 35 cell populations; (B) Heatmap, visualizing DEG by each cell cluster; (C) UMAP plot and dot plot, showing canonical cell markers as labeled clusters.

A.

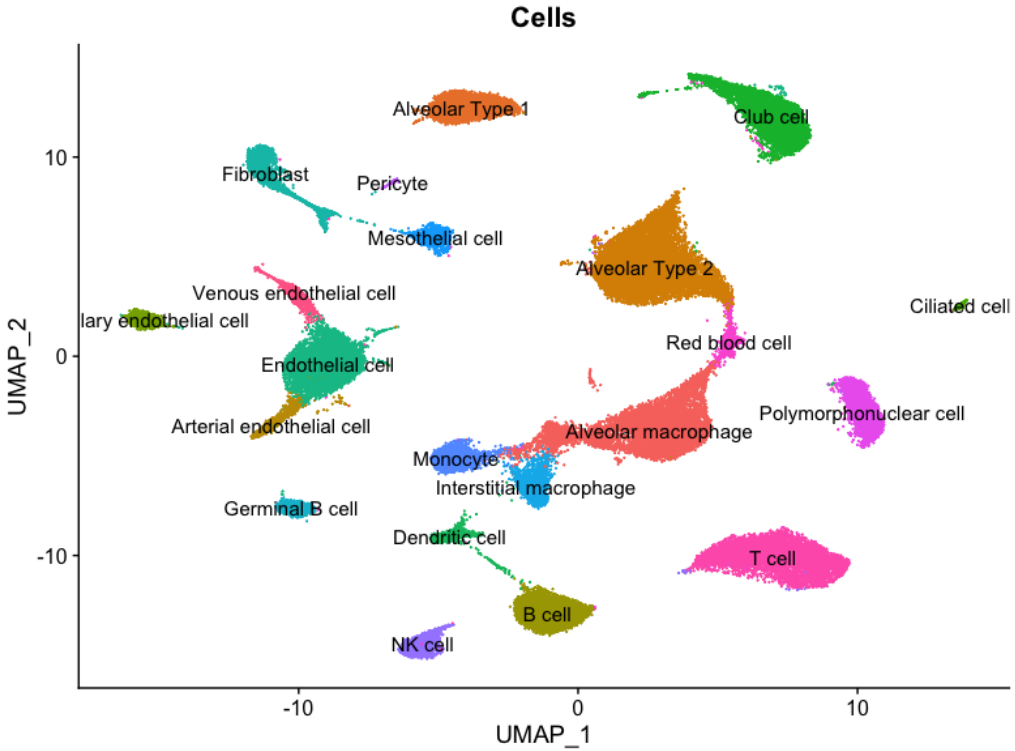

B.

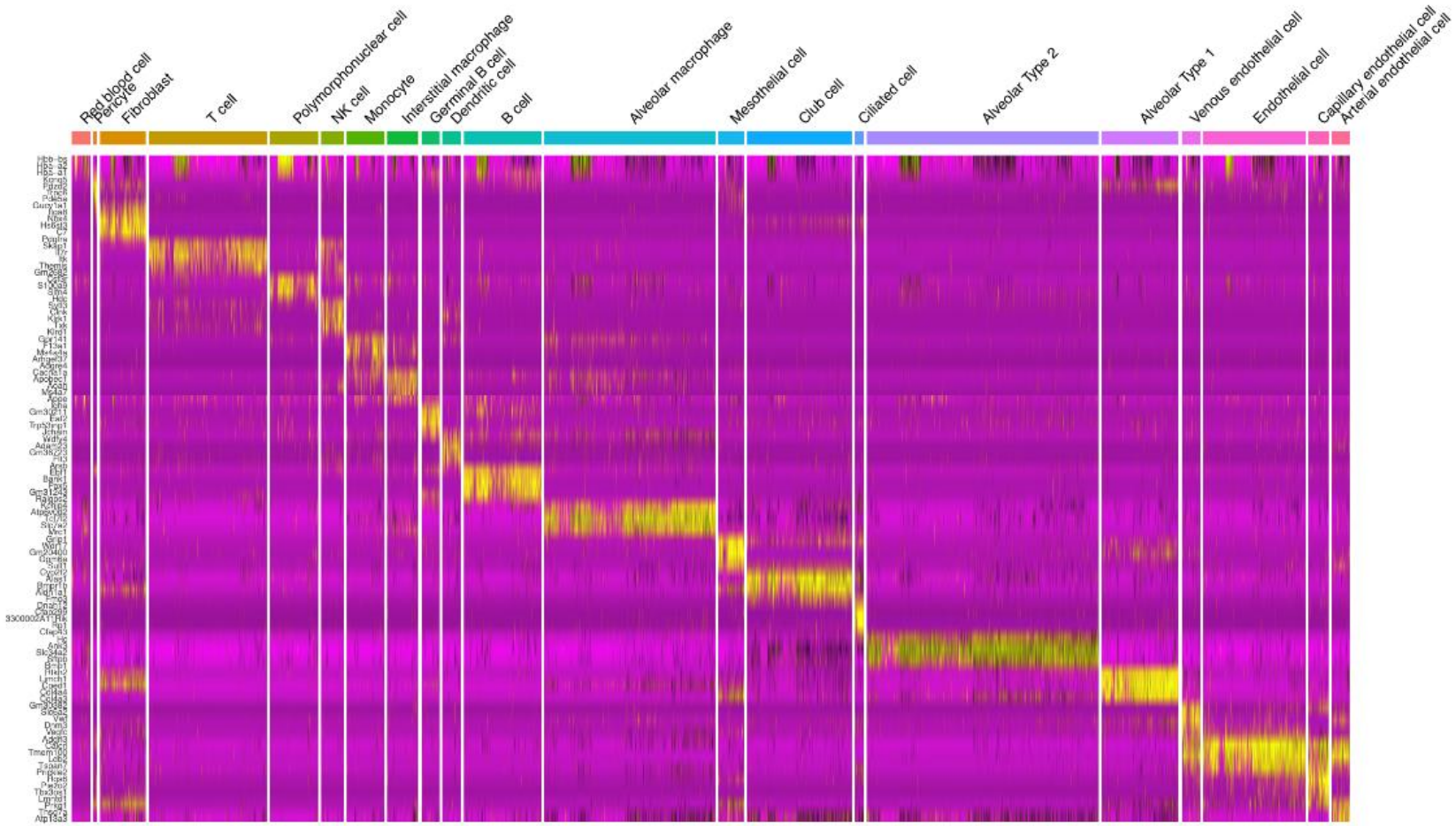
Red blood cell
Pericyte
Fibroblast
T cell
Polymorphonuclear cell
NK cell
Monocyte
Interstitial macrophage
Germinal B cell
Dendritic cell
B cell
Alveolar macrophage
Mesothelial cell
Club cell
Ciliated cell
Alveolar Type 2
Alveolar Type 1
Venous endothelial cell
Endothelial cell
Capillary endothelial cell
Arterial endothelial cell

C.

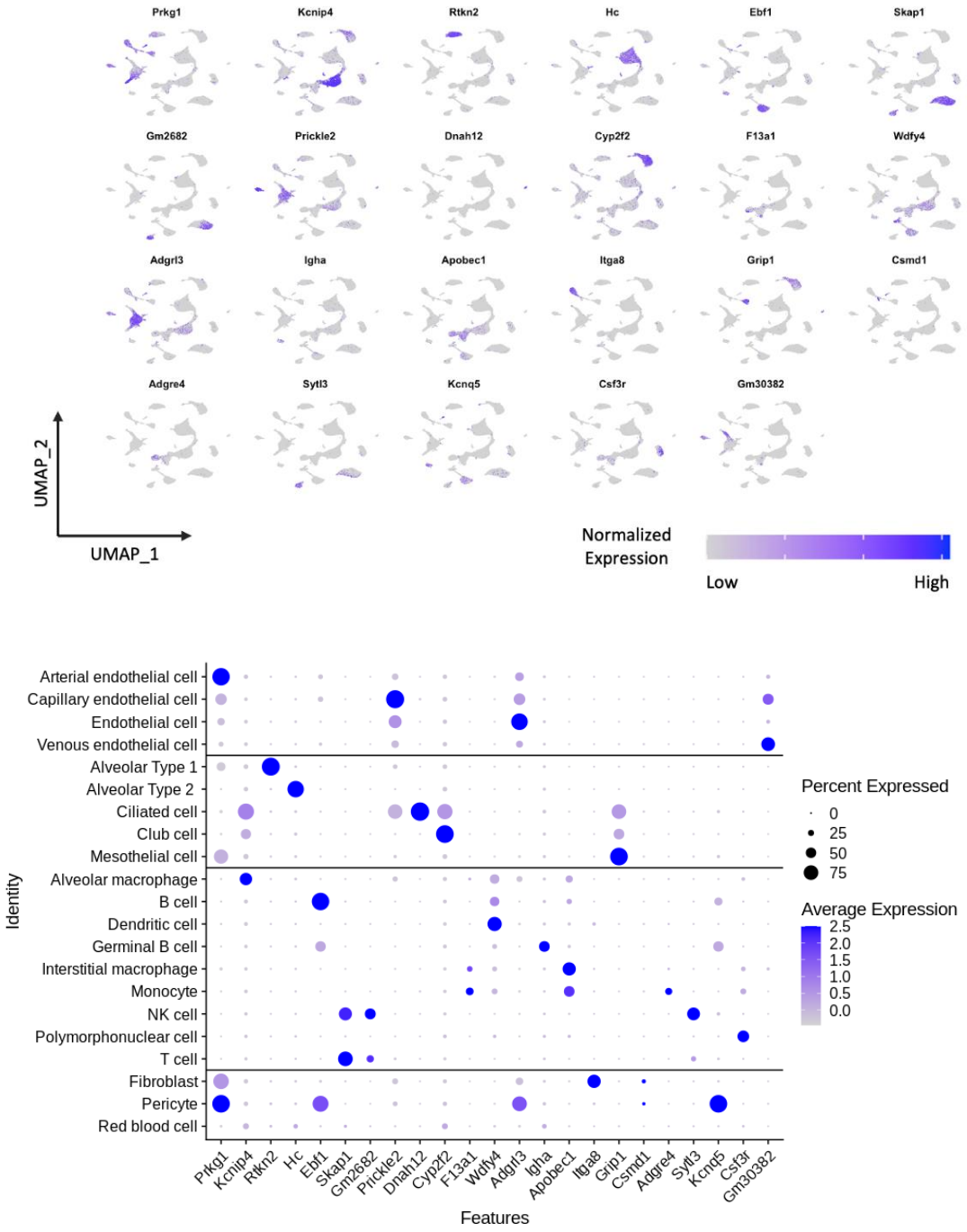
Prkg1
Kcnip4
Rtkn2
Hc
Ebf1
Skap1
Gm2682
Prickle2
Dnah12
Cyp2f2
F13a1
Wdfy4
Adgrl3
Igha
Apobec1
Itga8
Grip1
Csmd1
Adgre4
Sytl3
Kcnq5
Csf3r
Gm30382
UMAP_2
UMAP_1
Normalized Expression
Low
High
Arterial endothelial cell
Capillary endothelial cell
Endothelial cell
Venous endothelial cell
Alveolar Type 1
Alveolar Type 2
Ciliated cell
Club cell
Mesothelial cell
Alveolar macrophage
B cell
Dendritic cell
Germinal B cell
Interstitial macrophage
Monocyte
NK cell
Polymorphonuclear cell
T cell
Fibroblast
Pericyte
Red blood cell
Identity
Features
Percent Expressed
0
25
50
75
Average Expression
2.5
2.0
1.5
1.0
0.5
0.0

Figure 12. Distribution of cell types by treatment group: (A) UMAP showing that in all four groups the most common cell population was immune cells followed by epithelial cells and the most common cell type was type 2 alveolar cell; (B). Bar plot showing relative distribution of cellular composition among immune, endothelial, fibroblast, and epithelial cell populations; (C). In immune cell population, the proportions of the cell types varied most dynamically with treatment.

A.

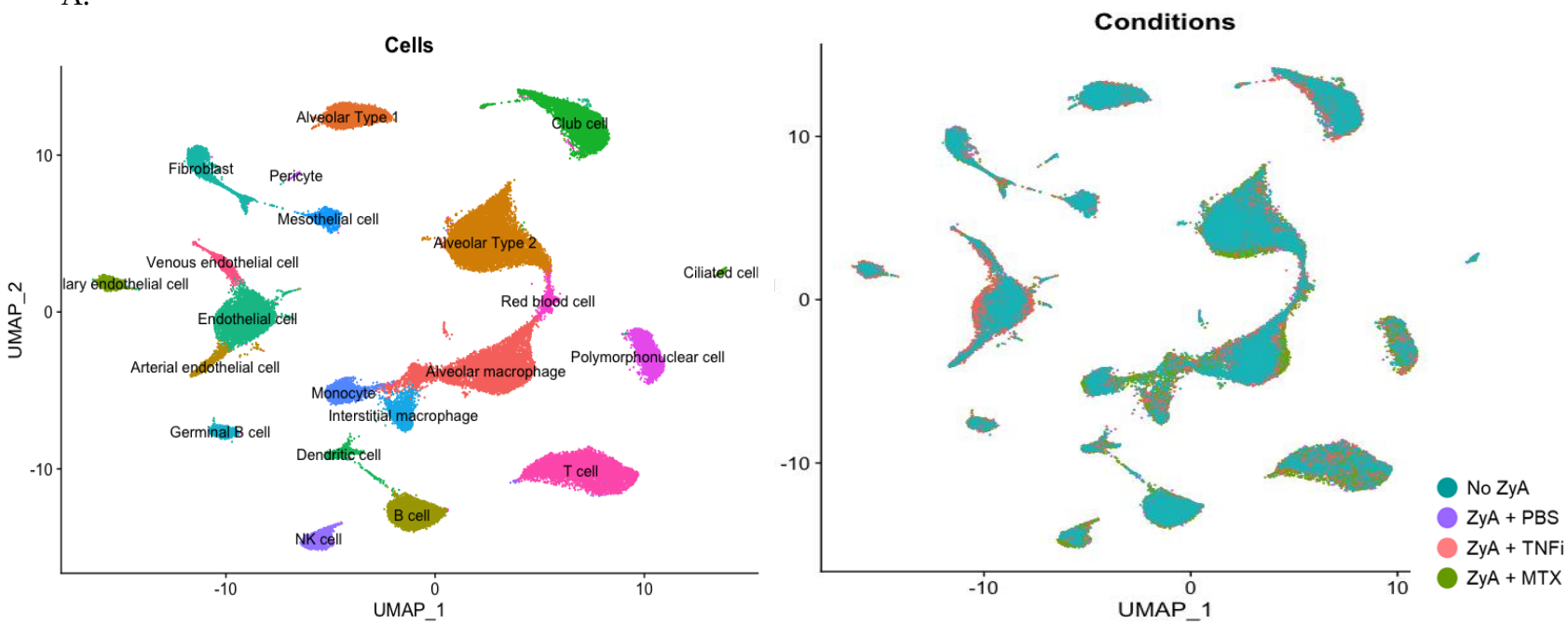

B.

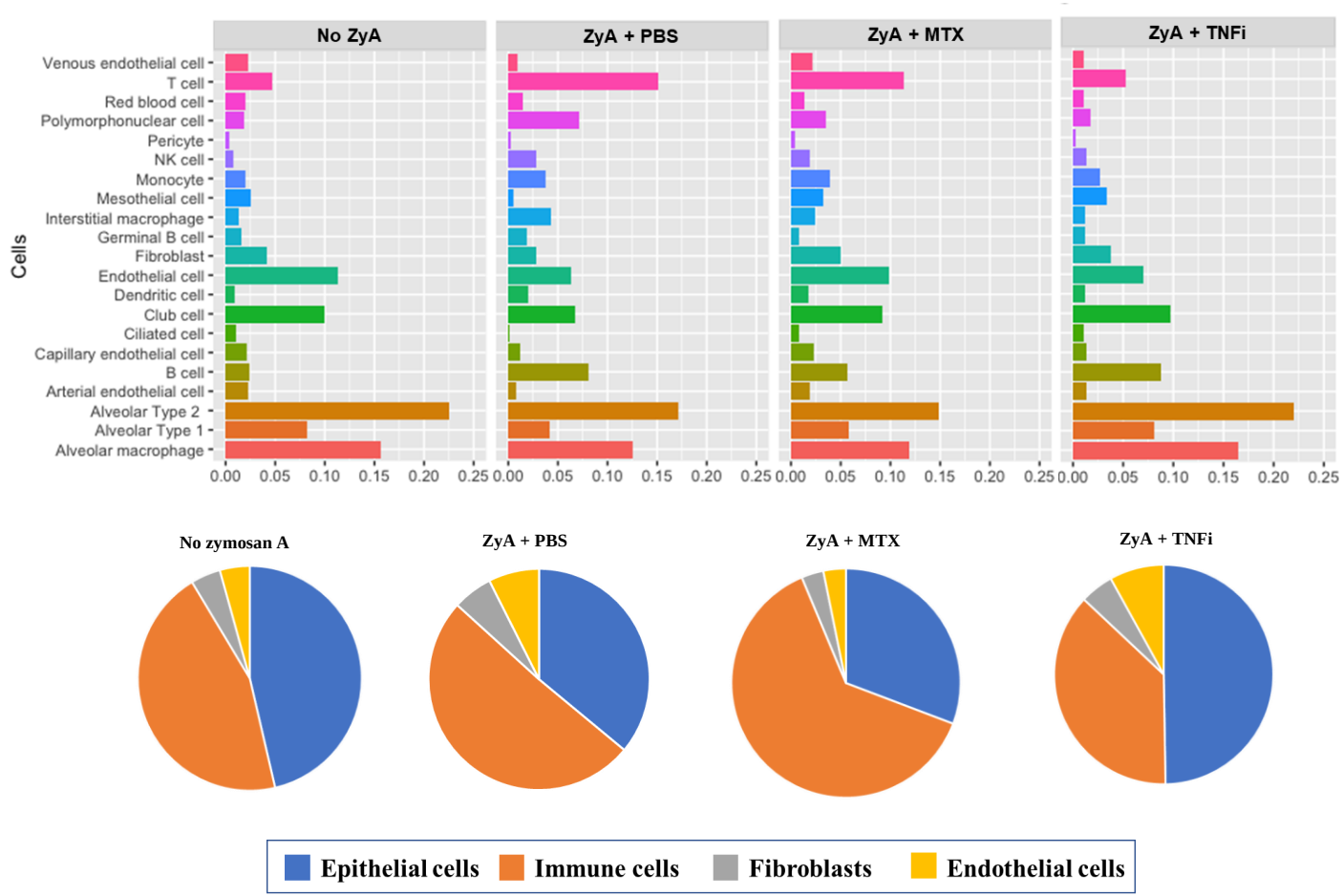
No ZyA
ZyA + PBS
ZyA + MTX
ZyA + TNFi
Cells
Venous endothelial cell
T cell
Red blood cell
Polymorphonuclear cell
Pericyte
NK cell
Monocyte
Mesothelial cell
Interstitial macrophage
Germinal B cell
Fibroblast
Endothelial cell
Dendritic cell
Club cell
Ciliated cell
Capillary endothelial cell
B cell
Arterial endothelial cell
Alveolar Type 2
Alveolar Type 1
Alveolar macrophage
0.00 0.05 0.10 0.15 0.20 0.25
No zymosan A
ZyA + PBS
ZyA + MTX
ZyA + TNFi
Epithelial cells
Immune cells
Fibroblasts
Endothelial cells

C.

(a) Immune cells

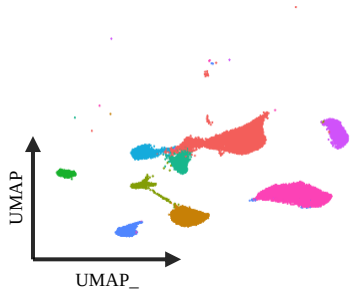

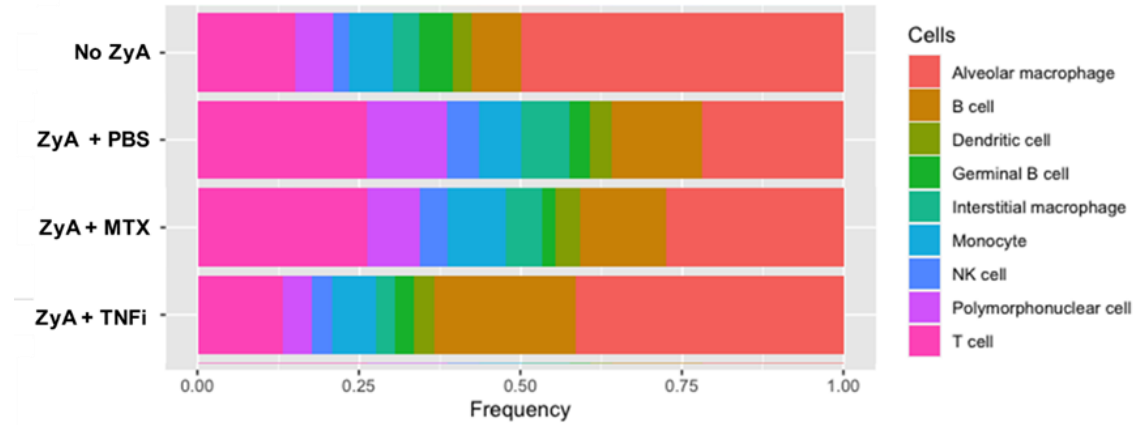

(b) Endothelial cells

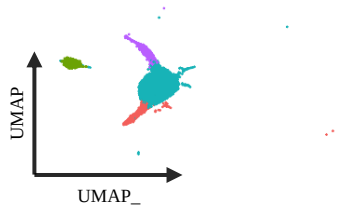

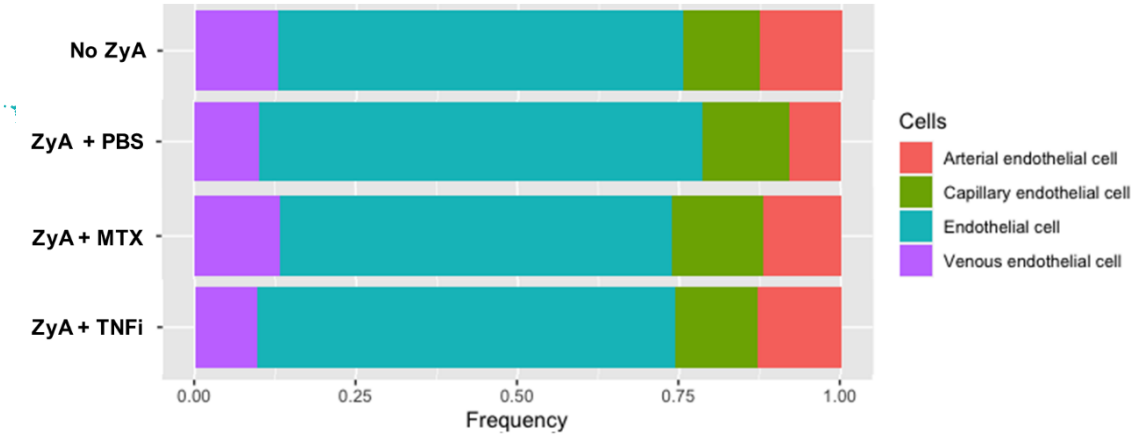

(c) Epithelial cells

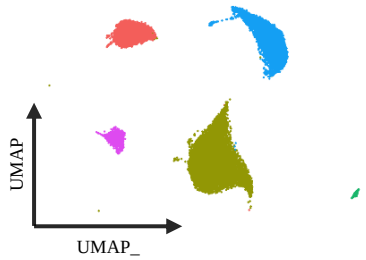

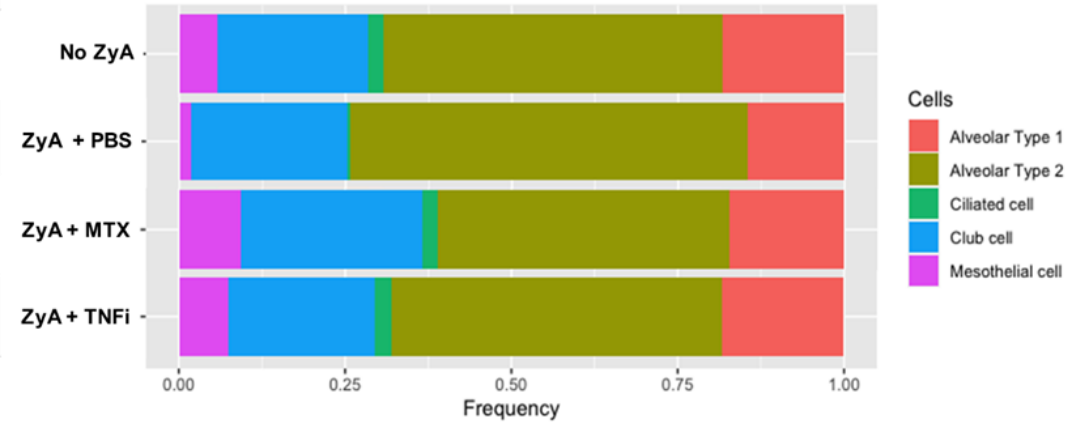

Figure 13. Distribution of (A) up-regulated genes and (B) down-regulated genes in immune cell population by cell type. Up-regulated genes were most frequently observed in alveolar macrophage.

A.

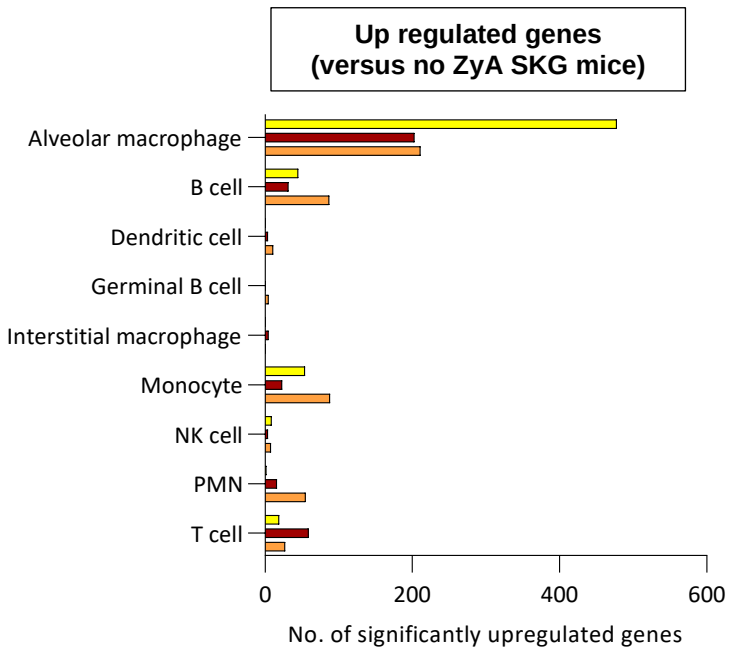

B.

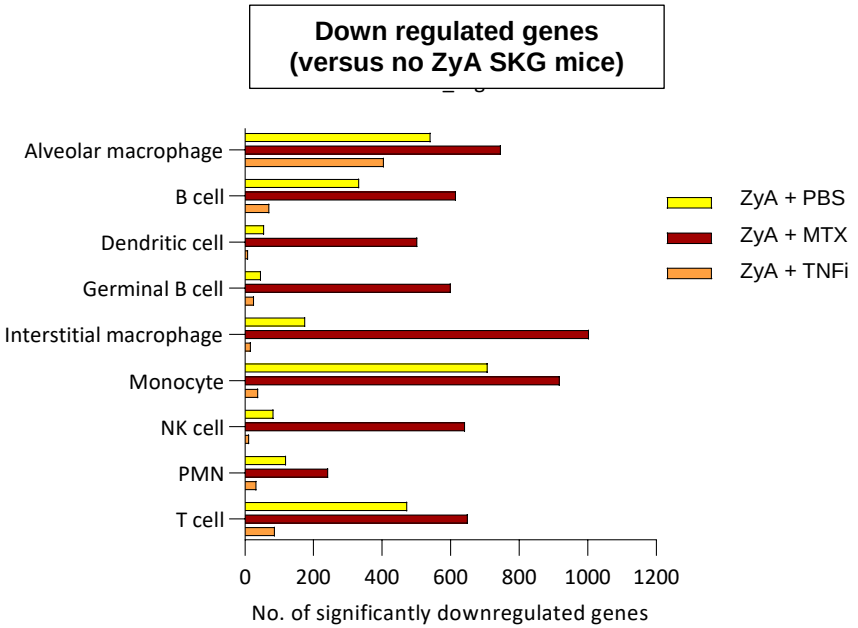

Figure 14. Gene expression changes from baseline in alveolar macrophages in SKG mice injected with zymosan A, by treatment group: (A) Heatmap indicates up- regulated and down-regulated genes of alveolar macrophages and enriched pathways derived from the MSigDB database; (B) Venn diagrams indicate up-regulated or down-regulated genes of alveolar macrophages and enriched gene pathways changed by methotrexate or TNFα inhibitor treatment only.

A.

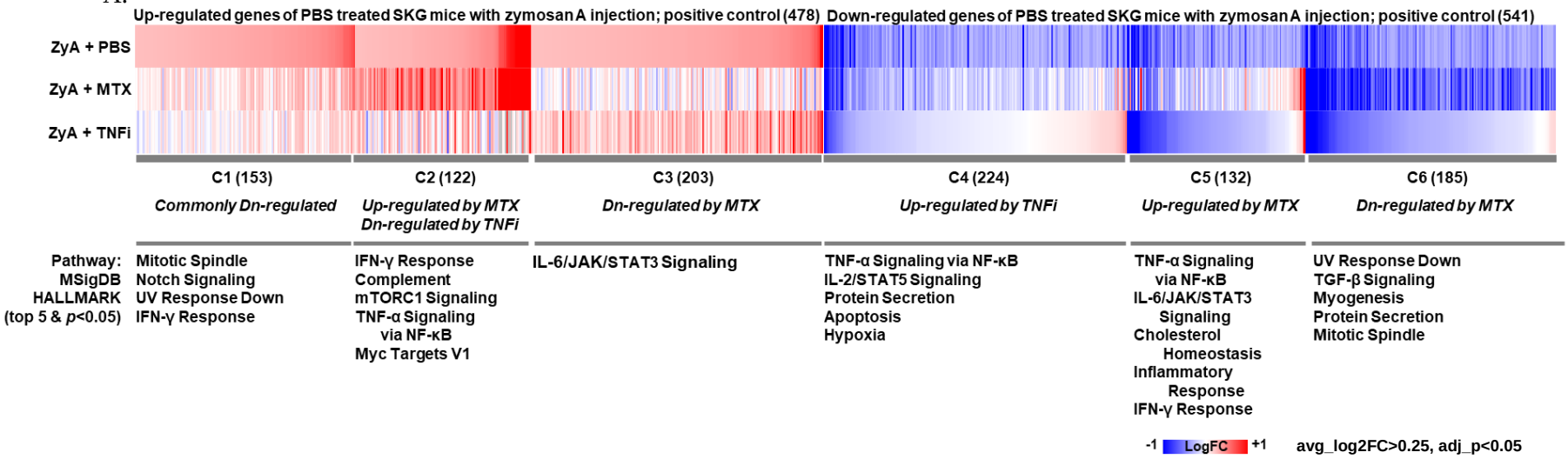

B.

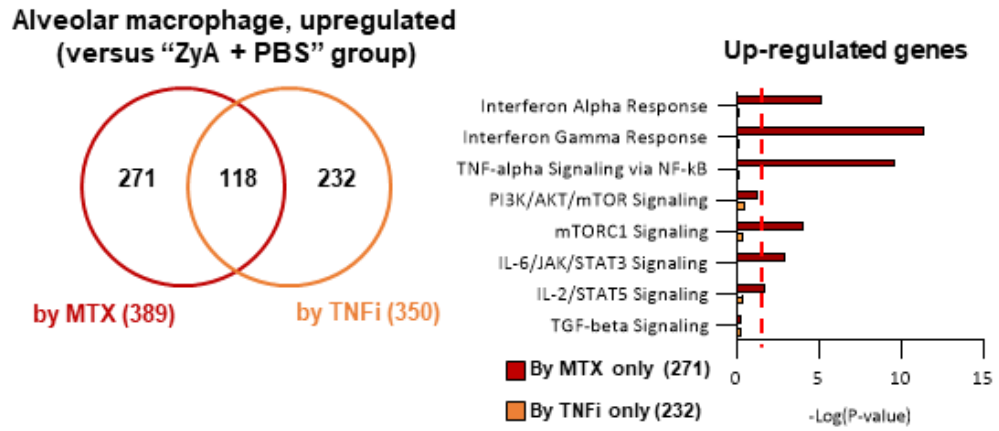
Alveolar macrophage, upregulated
(versus "ZyA + PBS" group)
271
118
232
by MTX (389)
by TNFi (350)
Up-regulated genes
Interferon Alpha Response
Interferon Gamma Response
TNF-alpha Signaling via NF-kB
PI3K/AKT/mTOR Signaling
mTORC1 Signaling
IL-6/JAK/STAT3 Signaling
IL-2/STAT5 Signaling
TGF-beta Signaling
By MTX only (271)
By TNFi only (232)
0
5
10
15
-Log(P-value)

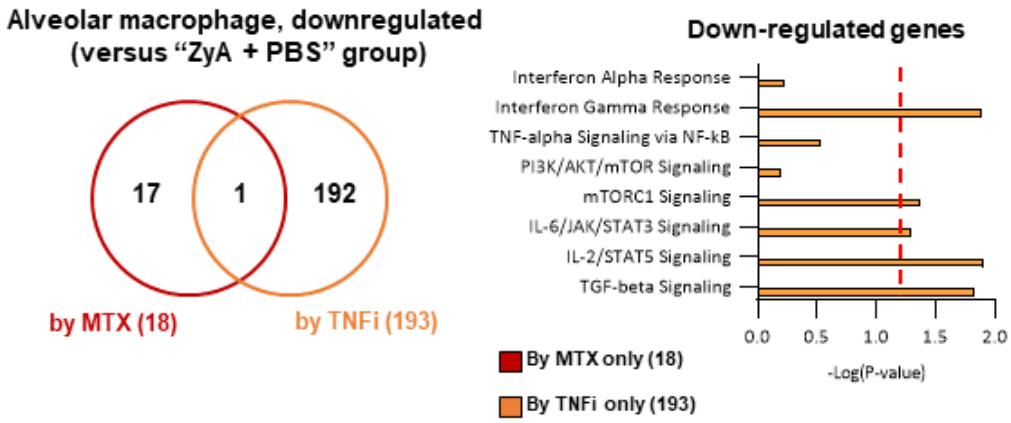
Alveolar macrophage, downregulated
(versus "ZyA + PBS" group)
17
1
192
by MTX (18)
by TNFi (193)
Down-regulated genes
Interferon Alpha Response
Interferon Gamma Response
TNF-alpha Signaling via NF-kB
PI3K/AKT/mTOR Signaling
mTORC1 Signaling
IL-6/JAK/STAT3 Signaling
IL-2/STAT5 Signaling
TGF-beta Signaling
By MTX only (18)
By TNFi only (193)
0.0
0.5
1.0
1.5
2.0
-Log(P-value)

Figure 15. Gene expression changes from baseline in T cells of SKG mice injected with zymosan A, by treatment group: (A) Heatmap indicates up- regulated and down-regulated genes of T cells and enriched pathways derived from the MSigDB database; (B) Venn diagrams indicate up-regulated or down-regulated genes of T cells and enriched gene pathways changed by methotrexate or TNFα inhibitor treatment only.

A.

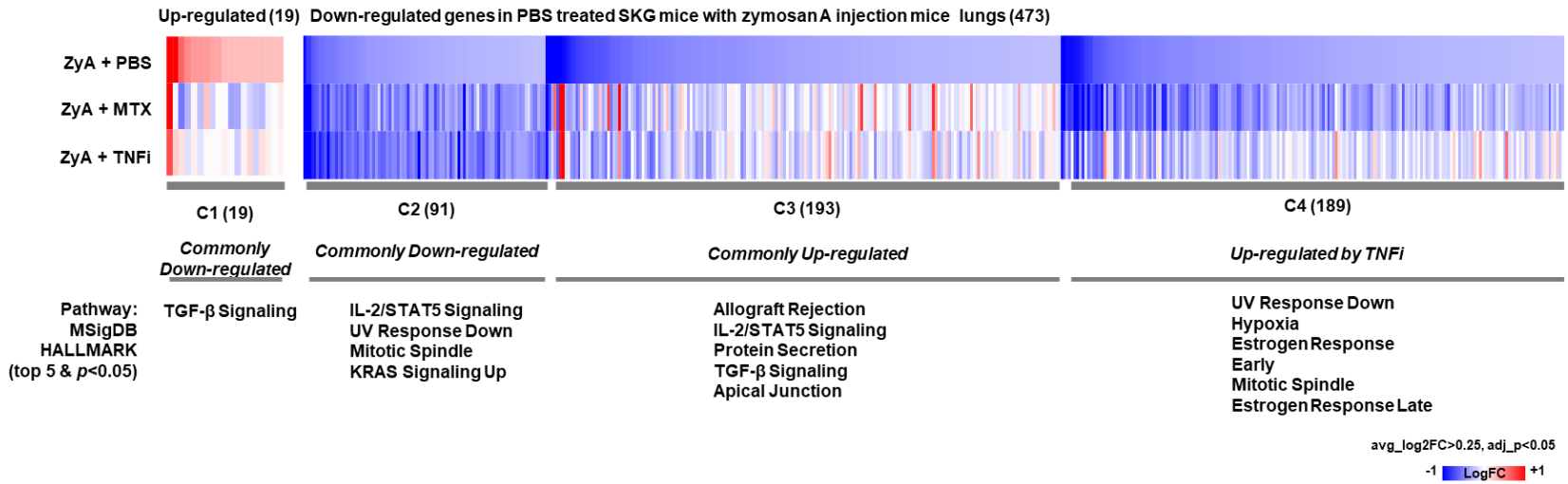

B.

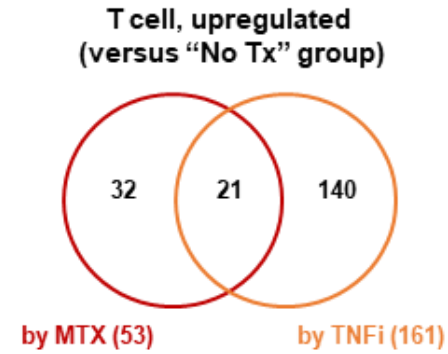
T cell, upregulated
(versus "No Tx" group)
32
21
140
by MTX (53)
by TNFi (161)

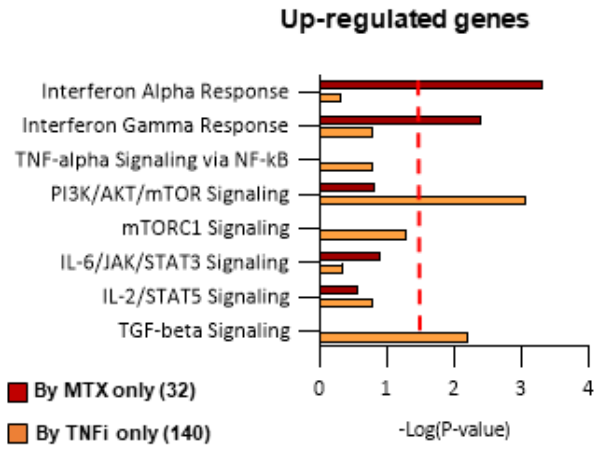
Up-regulated genes
Interferon Alpha Response
Interferon Gamma Response
TNF-alpha Signaling via NF-kB
PI3K/AKT/mTOR Signaling
mTORC1 Signaling
IL-6/JAK/STAT3 Signaling
IL-2/STAT5 Signaling
TGF-beta Signaling
0
1
2
3
4
By MTX only (32)
By TNFi only (140)
-Log(P-value)

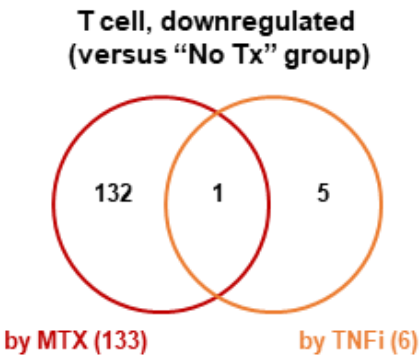
T cell, downregulated
(versus "No Tx" group)
132
1
5
by MTX (133)
by TNFi (6)

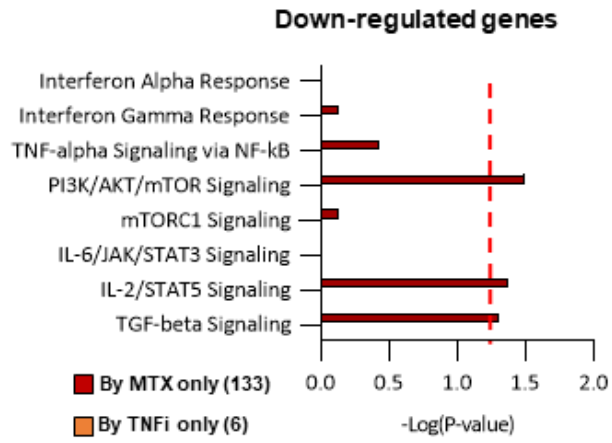
Down-regulated genes
Interferon Alpha Response
Interferon Gamma Response
TNF-alpha Signaling via NF-kB
PI3K/AKT/mTOR Signaling
mTORC1 Signaling
IL-6/JAK/STAT3 Signaling
IL-2/STAT5 Signaling
TGF-beta Signaling
0.0
0.5
1.0
1.5
2.0
By MTX only (133)
By TNFi only (6)
-Log(P-value)

Figure 16. Cellular composition of fibroblasts, by treatment group:(A) UMAP visualizes seven clusters of fibroblasts that were identified, with cell populations area colored as indicated by the legend: (B). Embedded UMAP and psi charts show distribution of cell populations. The proportions of clusters were dynamically changed by treatment.

A.

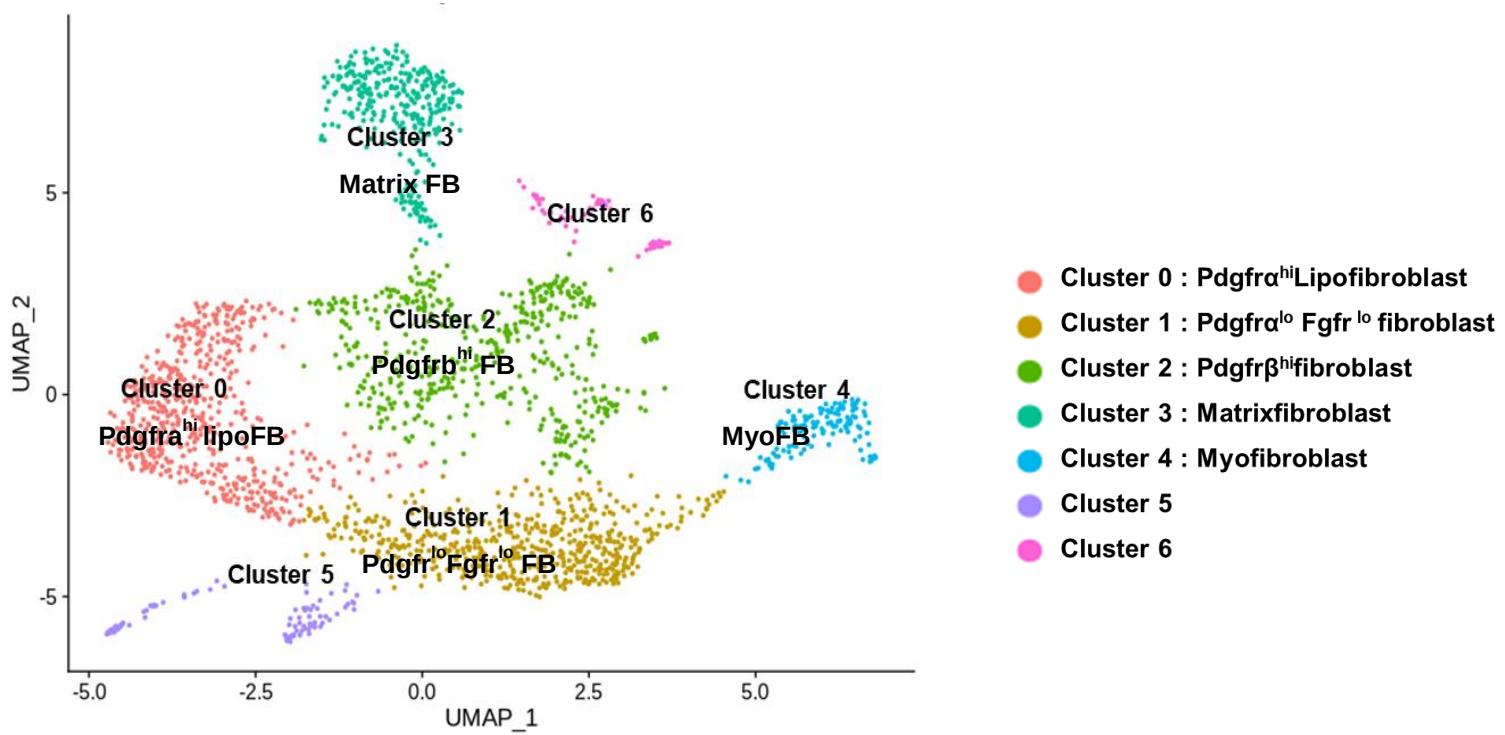

B.

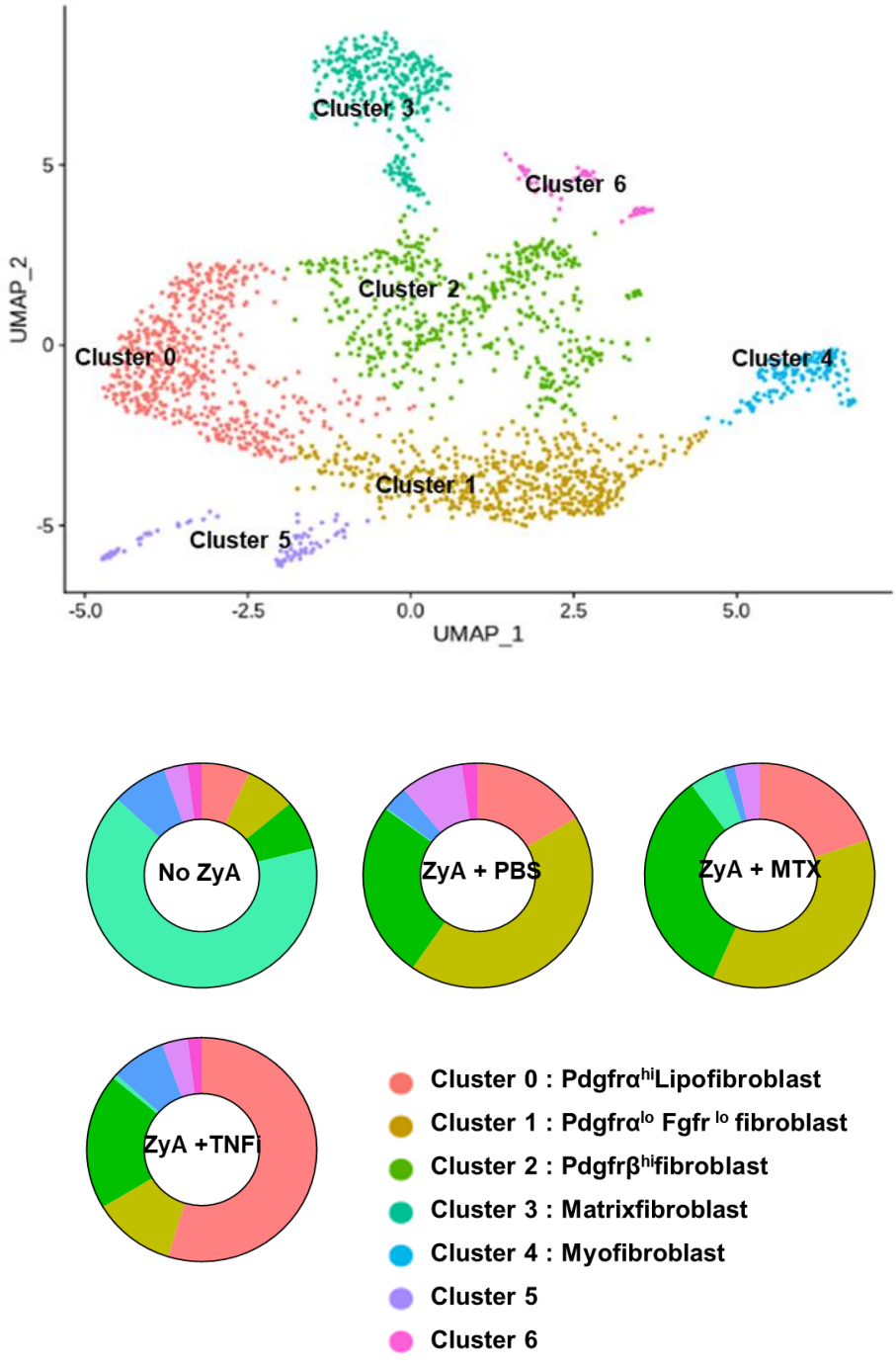
Cluster 3
Cluster 6
Cluster 2
Cluster 0
Cluster 4
Cluster 1
Cluster 5
UMAP_2
UMAP_1
5
0
-5
-5.0
-2.5
0.0
2.5
5.0
No ZyA
ZyA + PBS
ZyA + MTX
ZyA +TNFi
Cluster 0 : Pdgfrα^{hi}Lipofibroblast
Cluster 1 : Pdgfrα^{lo} Fgfr ^{lo} fibroblast
Cluster 2 : Pdgfrβ^{hi}fibroblast
Cluster 3 : Matrixfibroblast
Cluster 4 : Myofibroblast
Cluster 5
Cluster 6

Figure 17. Transcriptome perturbation signature with nintedanib to characterize fibroblast clusters: (A) Heatmap indicates intensity of concordance of gene expression of each cluster and down-regulated genes by nintedanib treatment using Ligand 1000 perturbation; (B). Bar chart shows expression of signature genes responsive to nintedanib by subcluster.

A.

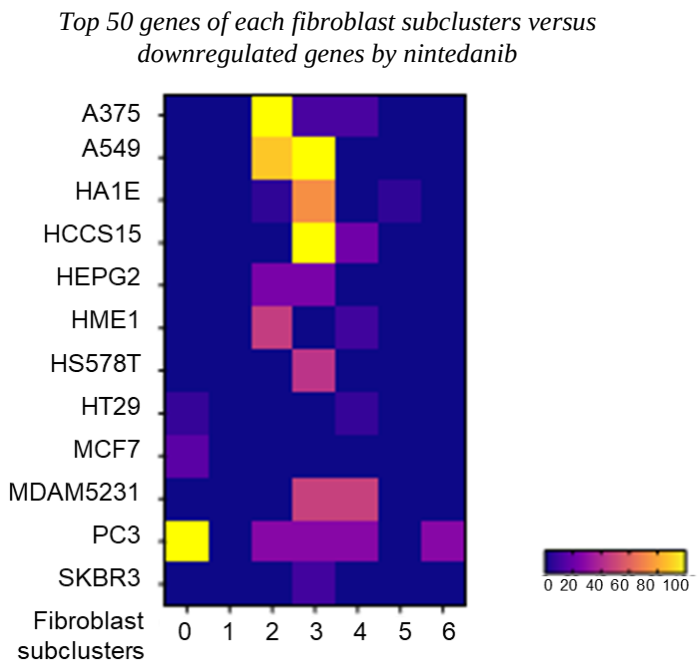

B.

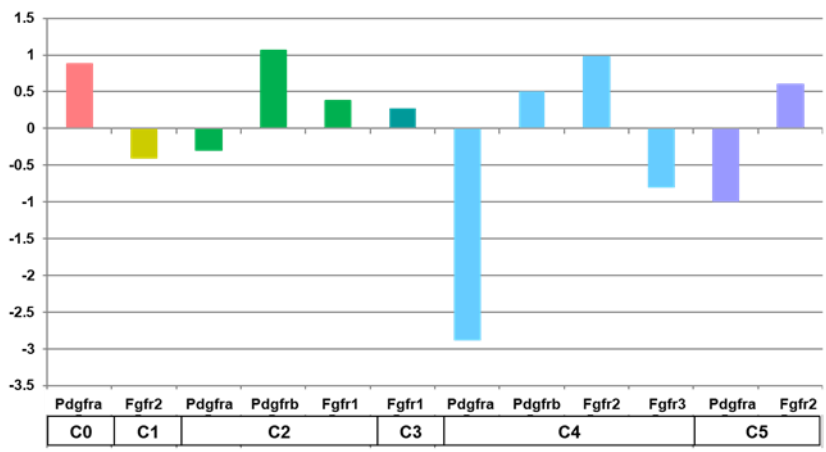

Figure 18. Cellular composition of alveolar epithelial cells, by treatment group: (A) UMAP visualizes six clusters of alveolar epithelial cells, with cell populations area colored as indicated by the legend; (B) Embedded UMAP and psi charts show distribution of cell populations. The proportions of cluster were dynamically changed by treatment. Cluster 3 is the unique cluster observed in SKG mice injected with zymosan A and treated with methotrexate.

A.

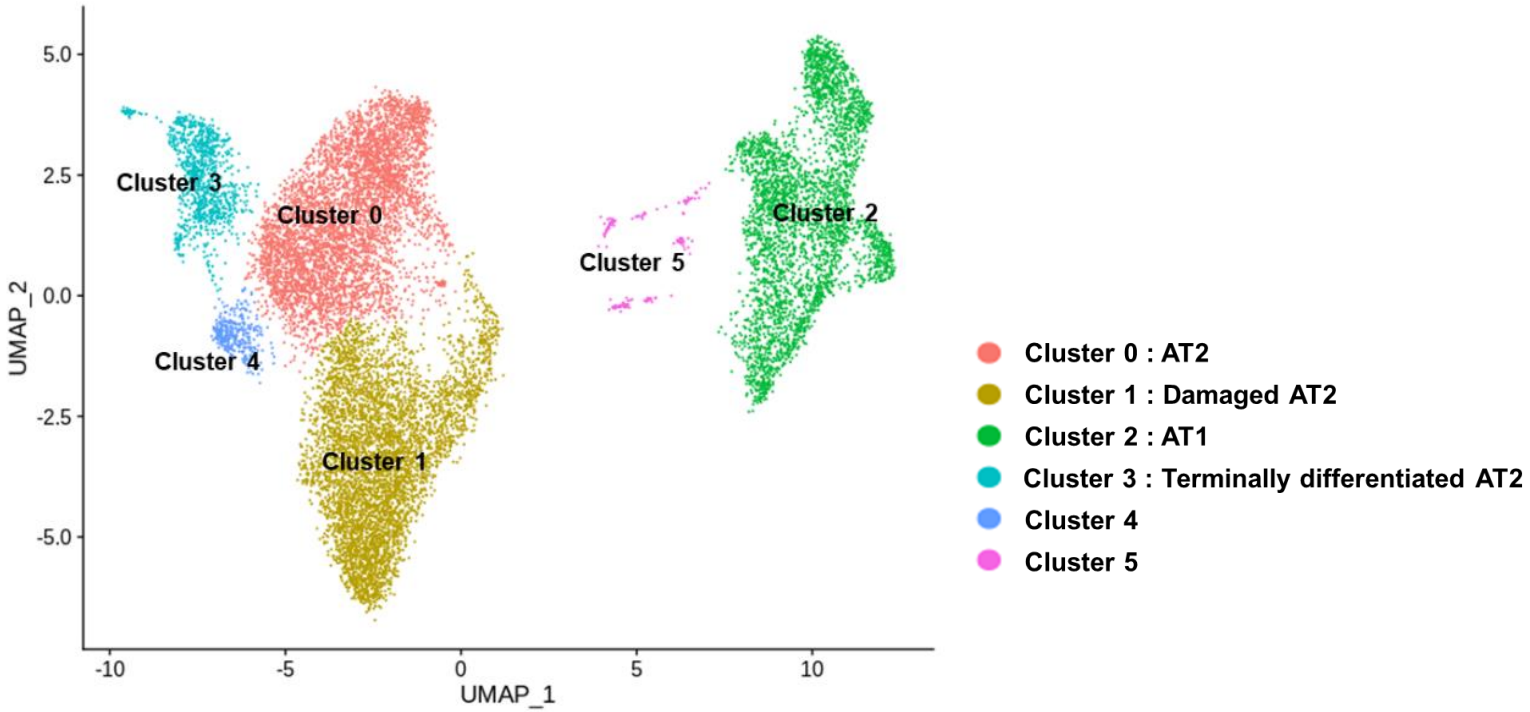

B.

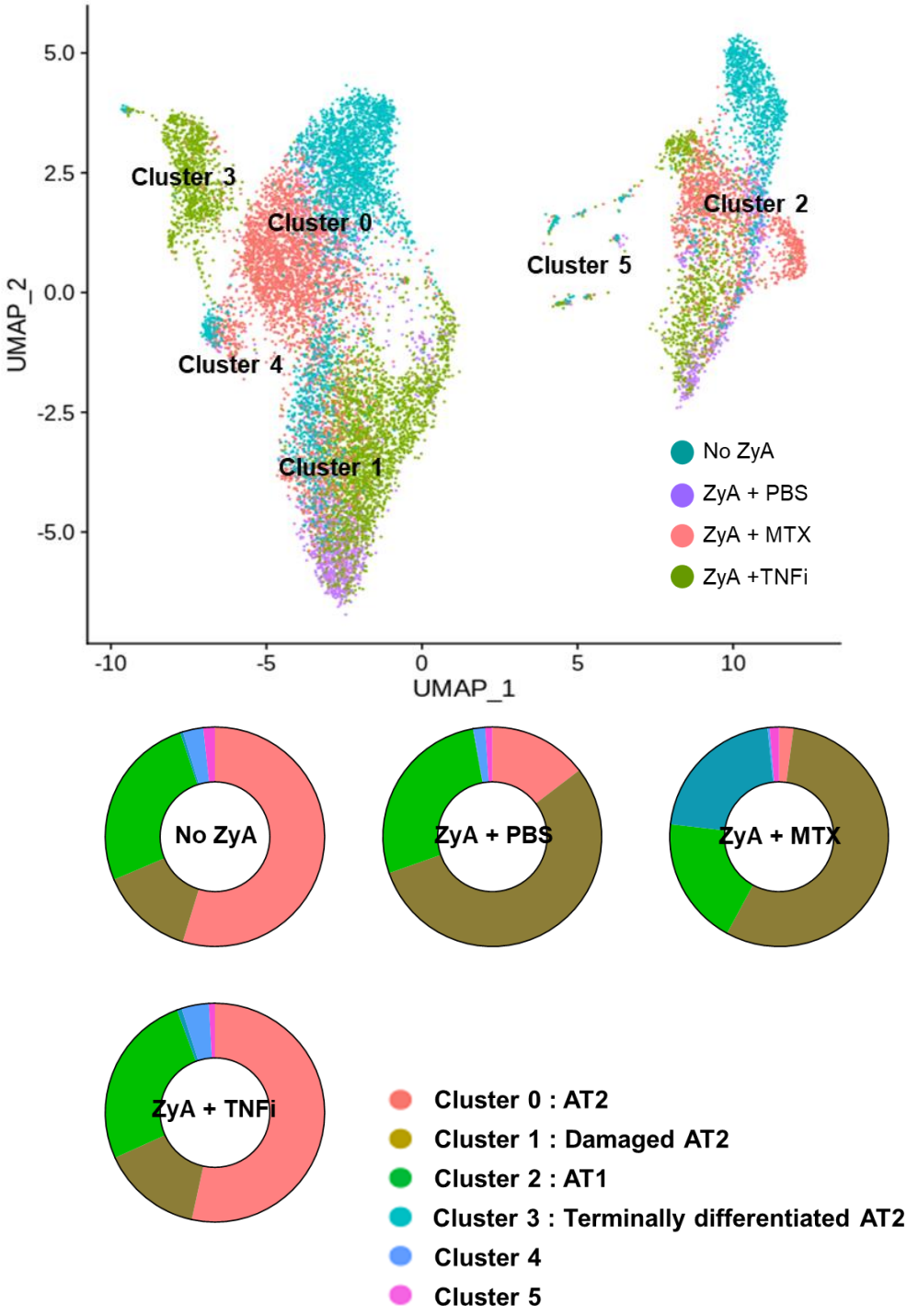
5.0
2.5
0.0
-2.5
-5.0
UMAP_2
-10
-5
0
5
10
UMAP_1
Cluster 3
Cluster 0
Cluster 4
Cluster 1
Cluster 5
Cluster 2
No ZyA
ZyA + PBS
ZyA + MTX
ZyA +TNFi
No ZyA
ZyA + PBS
ZyA + MTX
ZyA + TNFi
Cluster 0 : AT2
Cluster 1 : Damaged AT2
Cluster 2 : AT1
Cluster 3 : Terminally differentiated AT2
Cluster 4
Cluster 5

Figure 19. Perturbation signature with inflammatory cytokines and enrichment analysis of characteristics of alveolar cell clusters: (A) Heatmaps indicate intensity of concordance of gene expression of each cluster and up-regulated genes by ligand perturbation with cytokines, using Ligand 1000 perturbation;(B) Charts show enrichment analysis using derepressed gene set of Bmi1 knockout mice.

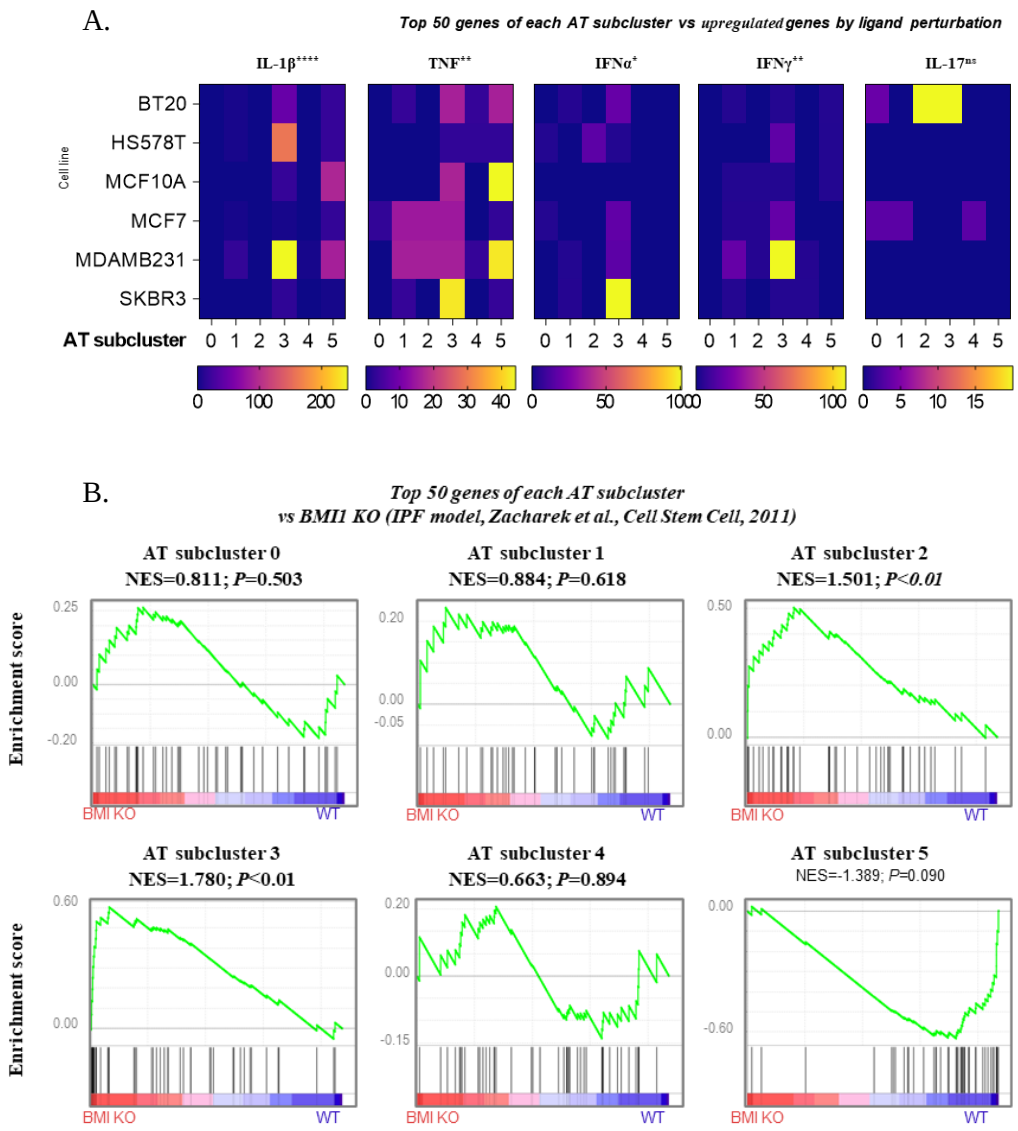

CONCLUSIONS

The current study aimed to study the effect of DMARDs on lungs in RA-ILD. This study was organized into two parts: the first part was conducted to assess the effect of DMARDs on lungs in the aspect of clinical course using a prospective cohort, and the second part was conducted to investigate the effect of DMARDs on lungs in the aspect of the transcriptome using a murine disease model.

In the first part, using a prospective cohort of patients with RAILD, methotrexate treatment was not associated with aggravation of lung function or lung fibrosis overall. However, there was significant change in fibrosis on CT scans in patients with extensive fibrosis, defined as ≥30% abnormal lung lesion involvement of the whole lung. This result suggests that methotrexate can further exacerbate lung damage when the preexisting lung damage is profound.

Interestingly, in the second part, the disease animal model experiment, PBS-treated SKG mice with zymosan A injection showed transcriptome changes in a direction similar to that of methotrexate-treated SKG mice with zymosan A injection, but histologically evident lung lesions were observed only in the latter. This result could be interpreted as methotrexate-accelerated lung inflammation. Of note, among AT2 cells of methotrexate- treated SKG mice with zymosan A injection, there was a unique cluster that was not observed in other treatment groups. The AT2 cells in this cluster showed significantly reduced regenerative capacity and were in a fully differentiated form.

Methotrexate is the cornerstone drug in treatment of rheumatoid arthritis[1]. It was initially developed as a folate pathway antagonist by inhibiting dihydrofolate

reductase at a high dose for treating leukemia.[67] In rheumatoid arthritis, methotrexate is used in a low dose; it is supposed that methotrexate engages via the adenosine signaling pathway.[67, 68] Methotrexate blocks the enzyme 5-aminomidazole-4-carboxamide ribonucleotide (AICAR) transformylase (ATIC), and increased AICAR inhibits intracellular adenosine deaminase. Decreased adenosine deaminase leads to an increased level of adenosine, which is transported out of the cell by the extracellular nucleoside transporter (ENT1) and stimulated extracellular adenosine receptor.

Adenosine seems to exhibit a pleomorphic effect on the lung; it has a different role during acute and chronic stages of lung injury.[69] Mice without the adenosine A2B receptor were less susceptible to bleomycin-induced pneumonitis[70], and adenosine A2A receptor agonists reduce ischemia-reperfusion injury after lung transplantation.[69, 71, 72] In other studies, adenosine A2B receptor stimulation has been reported to drive the differentiation of pulmonary fibrosis, and mice deficient in adenosine deaminase exhibit increased fibroblast numbers and accumulation of α-smooth muscle actin.[69, 73, 74] Hypoxia-inducible factor 1α (HIF-1α) enhances adenosine A1B receptor (ADORA1B) expression to regulate M2 macrophage differentiation and production of profibrotic mediators.[50, 70] Of note, caffeine administration in hyperoxia-exposed newborn mice was associated with lung hypoplasia, with increased epithelial cell apoptosis and decreased numbers of type 2 alveolar cells.[75]

There have been controversies about whether methotrexate treatment is associated with the development or acceleration of lung disease.[19] A recent meta-analysis and large-scale case control study indicated that association of methotrexate

exposure with. development of fibrosing ILD is not affirmative[18, 27, 76, 77]; rather, it revealed that methotrexate treatment is associated with improved survival. Recent results of the effect of methotrexate on the lungs were studies on whether ILD is newly diagnosed or developed in patients receiving methotrexate[18, 27, 76] By contrast, the most recent previous report of negative effects of methotrexate on the lungs involved patients with preexisting ILD.[38, 78-80]

In the current study, alveolar cells of methotrexate-treated SKG mice with zymosan A injection were skewed in clusters 1 and 3. Identification of the subtype distinguishing genes of cluster 1 revealed an association with decreased apoptosis such as Iigp1 and safb. Interferon-inducible GTPase 1 (Iipg1) is known to inhibit apoptosis and promote lysosomal destruction of autophagosome in response to interferon-beta[81], and scaffold attachment factor B1(Sab) is known to be a negative regulator of cell proliferation[82]. The most distinctive genes of cluster 3 were associated with senescence and late-type alveolar cell markers (scd1, H2-Aa, H2-D1, H2-Eb1, Lcn2, Sftpc, and Sftpd),[57, 61, 63] and further enriched with Bmi1 knockout mouse genes[65]. With previous and current study results, it might be speculated that type 2 alveolar cells are less prone to regenerate to type 1 alveolar cells with increased adenosine in the inflammatory milieu. Results of the KORAIL cohort also indicated that patients with extensive preexisting ILD had worse fibrosis scores with methotrexate treatment during follow-up periods. However, to confirm this hypothesis, further studies are warranted.

There were several limitations in the current study. First, the number of patients included in the analysis was small, and most of the patients of the KORAIL cohort had less than 10% of lung involvement in chest CT scans. Patients with extensive

involvement showed significant increase in fibrosis scores, but there were only 19 such patients. This study result should be further validated in large numbers of patients. Second, histological lung inflammation was not fully developed in a group of zymosan A-injected SKG mice with PBS treatment, corresponding to a positive control group. A more extended experimental period, probably more than 20-24 weeks, might be needed to observe overt pneumonitis. However, in the current study, even at twelve weeks, although the histological change was not evident, there was a significant change in transcriptome compared with SKG mice without the zymosan A injection, corresponding to a negative control. We detected very early transcriptome change, which results from studies that can only be performed in animal models and is very difficult to obtain in human studies. Finally, the current study did not encompass the effect of medication dose. Medications—especially methotrexate, as stated before—may have a different effect according to dose via different primary mechanisms of action.[67, 83] In the current study, only one dose of methotrexate or TNFα inhibitor was used in an animal study. The dose and total exposure duration of methotrexate were various in the KORAIL cohort. A 7.5 mg/kg dose of methotrexate used in animal models corresponds to a dose of approximately 0.6 mg/kg in humans[84], which is higher than the low-dose methotrexate used in RA. However, previous research reported that a daily 10mg/kg intraperitoneal injection effectively abrogated arthritis in SKG mice,[85] and a daily 2.5 mg/kg intraperitoneal injection alleviated arthritis most effectively in collagen-induced arthritis (CIA) mice.[86] Therefore, we used 7.5 mg/kg twice a week of methotrexate intraperitoneally, corresponding approximately to daily 2.1 mg/kg. In the KORAIL cohort, although the methotrexate dose was various among patients, we classified patients with

methotrexate treatment as those who had taken methotrexate at least six months consecutively within a three-year observational period, which was a sufficient period considering that the effect of DMARDs begins at least two weeks after administration.

In summary, administration of methotrexate worsened the lung fibrosis score in patients with severe RA-ILD, defined as ≥30% lung involvement on a chest CT scan. In an animal model of RA-ILD, namely SKG mice with a zymosan A injection, administration of methotrexate exacerbated pneumonitis due to results of the inflammation response and mitigated regenerative capacity of AT2 cells.

Bibliography

1. Aletaha D, Smolen JS. Diagnosis and Management of Rheumatoid Arthritis: A Review. *JAMA* 2018;320(13):1360-72.

2. Spagnolo P, Distler O, Ryerson CJ, et al. Mechanisms of progressive fibrosis in connective tissue disease (CTD)-associated interstitial lung diseases (ILDs). *Annals of the Rheumatic Diseases* 2020:annrheumdis-202.

3. Hyldgaard C, Hilberg O, Pedersen AB, et al. A population-based cohort study of rheumatoid arthritis-associated interstitial lung disease: comorbidity and mortality. *Annals of the Rheumatic Diseases* 2017;76(10):1700-6.

4. Turesson C. Extra-articular rheumatoid arthritis. *Curr Opin Rheumatol* 2013;25(3):360-6.

5. McDermott GC, Doyle TJ, Sparks JA. Interstitial lung disease throughout the rheumatoid arthritis disease course. *Curr Opin Rheumatol* 2021;33(3):284-91.

6. Kadura S, Raghu G. Rheumatoid arthritis-interstitial lung disease: manifestations and current concepts in pathogenesis and management. *European Respiratory Review* 2021;30(160):210011.

7. Sparks JA, Jin Y, Cho SK, et al. Prevalence, incidence and cause-specific mortality of rheumatoid arthritis-associated interstitial lung disease among older rheumatoid arthritis patients. *Rheumatology (Oxford)* 2021.

8. Huang S, Doyle TJ, Hammer MM, et al. Rheumatoid arthritis-related lung disease detected on clinical chest computed tomography imaging: Prevalence, risk factors, and impact on mortality. *Semin Arthritis Rheum* 2020;50(6):1216-25.

9. Huang S, Kronzer VL, Dellaripa PF, et al. Rheumatoid Arthritis–Associated Interstitial Lung Disease: Current Update on Prevalence, Risk Factors, and Pharmacologic Treatment. *Current Treatment Options in Rheumatology* 2020;6(4):337-53.

10. Raimundo K, Solomon JJ, Olson AL, et al. Rheumatoid Arthritis–Interstitial Lung Disease in the United States: Prevalence, Incidence, and Healthcare Costs and Mortality. *The Journal of Rheumatology* 2019;46(4):360-9.

11. Duarte AC, Porter JC, Leandro MJ. The lung in a cohort of rheumatoid arthritis patients—an overview of different types of involvement and treatment. *Rheumatology* 2019;58(11):2031-8.

12. Brown KK, Martinez FJ, Walsh SLF, et al. The natural history of progressive fibrosing interstitial lung diseases. *European Respiratory Journal* 2020;55(6):2000085.

13. Fischer A, Distler J. Progressive fibrosing interstitial lung disease associated with systemic autoimmune diseases. *Clinical Rheumatology* 2019;38(10):2673-81.

14. Wongkarnjana A, Ryerson CJ. Progressive fibrosing interstitial lung disease: we know it behaves badly, but what does that mean? *European Respiratory Journal* 2020;55(6):2000894.

15. Anderson J, Caplan L, Yazdany J, et al. Rheumatoid arthritis disease activity measures: American College of Rheumatology recommendations for use in clinical practice. *Arthritis Care & Research* 2012;64(5):640-7.

16. Smolen JS, Landewé RBM, Bijlsma JWJ, et al. EULAR recommendations for the management of rheumatoid arthritis with synthetic and biological disease-

modifying antirheumatic drugs: 2019 update. *Annals of the Rheumatic Diseases* 2020;79(6):685-99.

17. Akiyama M, Kaneko Y, Yamaoka K, Kondo H, Takeuchi T. Association of disease activity with acute exacerbation of interstitial lung disease during tocilizumab treatment in patients with rheumatoid arthritis: a retrospective, case–control study. *Rheumatology International* 2016;36(6):881-9.

18. Kiely P, Busby AD, Nikiphorou E, et al. Is incident rheumatoid arthritis interstitial lung disease associated with methotrexate treatment? Results from a multivariate analysis in the ERAS and ERAN inception cohorts. *BMJ Open* 2019;9(5):e028466.

19. Fragoulis GE, Conway R, Nikiphorou E. Methotrexate and interstitial lung disease: controversies and questions. A narrative review of the literature. *Rheumatology* 2019;58(11):1900-6.

20. Juge PA, Lee JS, Lau J, et al. Methotrexate and rheumatoid arthritis associated interstitial lung disease. *Eur Respir J* 2020.

21. Wu EK, Ambrosini RD, Kottmann RM, Ritchlin CT, Schwarz EM, Rahimi H. Reinterpreting Evidence of Rheumatoid Arthritis-Associated Interstitial Lung Disease to Understand Etiology. *Curr Rheumatol Rev* 2019;15(4):277-89.

22. Malengier-Devlies B, Decaesteker T, Dekoster K, et al. Lung Functioning and Inflammation in a Mouse Model of Systemic Juvenile Idiopathic Arthritis. *Front Immunol* 2021;12:642778.

23. Song LN, Kong XD, Wang HJ, Zhan LB. Establishment of a Rat Adjuvant Arthritis-Interstitial Lung Disease Model. *Biomed Res Int* 2016;2016:2970783.

24. Cottin V, Hirani NA, Hotchkin DL, et al. Presentation, diagnosis and clinical course of the spectrum of progressive-fibrosing interstitial lung diseases. *European Respiratory Review* 2018;27(150):180076.

25. Flaherty KR, Wells AU, Cottin V, et al. Nintedanib in Progressive Fibrosing Interstitial Lung Diseases. *New England Journal of Medicine* 2019;381(18):1718-27.

26. Tashkin DP, Elashoff R, Clements PJ, et al. Cyclophosphamide versus Placebo in Scleroderma Lung Disease. *New England Journal of Medicine* 2006;354(25):2655-66.

27. Ibfelt EH, Jacobsen RK, Kopp TI, et al. Methotrexate and risk of interstitial lung disease and respiratory failure in rheumatoid arthritis: a nationwide population-based study. *Rheumatology* 2021;60(1):346-52.

28. England BR, Hershberger D. Management issues in rheumatoid arthritis-associated interstitial lung disease. *Curr Opin Rheumatol* 2020;32(3):255-63.

29. Conway R, Low C, Coughlan RJ, O'Donnell MJ, Carey JJ. Methotrexate use and risk of lung disease in psoriasis, psoriatic arthritis, and inflammatory bowel disease: systematic literature review and meta-analysis of randomised controlled trials. *BMJ* 2015;350(mar13 17):h1269-h.

30. Conway R, Low C, Coughlan RJ, O'Donnell MJ, Carey JJ. Methotrexate and Lung Disease in Rheumatoid Arthritis: A Meta-Analysis of Randomized Controlled Trials. *Arthritis & Rheumatology* 2014;66(4):803-12.

31. Sparks JA, Dellaripa PF, Glynn RJ, et al. Pulmonary Adverse Events in Patients Receiving Low-Dose Methotrexate in the Randomized, Double-Blind,

Placebo-Controlled Cardiovascular Inflammation Reduction Trial. *Arthritis & Rheumatology* 2020;72(12):2065-71.

32. Ridker PM, Everett BM, Pradhan A, et al. Low-Dose Methotrexate for the Prevention of Atherosclerotic Events. *New England Journal of Medicine* 2019;380(8):752-62.

33. Solomon JJ, Chung JH, Cosgrove GP, et al. Predictors of mortality in rheumatoid arthritis-associated interstitial lung disease. *European Respiratory Journal* 2016;47(2):588-96.

34. Qiu M, Jiang J, Nian X, et al. Factors associated with mortality in rheumatoid arthritis-associated interstitial lung disease: a systematic review and meta-analysis. *Respiratory Research* 2021;22(1).

35. Nurmi HM, Purokivi MK, Kärkkäinen MS, Kettunen H-P, Selander TA, Kaarteenaho RL. Are risk predicting models useful for estimating survival of patients with rheumatoid arthritis-associated interstitial lung disease? *BMC Pulmonary Medicine* 2017;17(1).

36. Morisset J, Vittinghoff E, Lee BY, et al. The performance of the GAP model in patients with rheumatoid arthritis associated interstitial lung disease. *Respiratory Medicine* 2017;127:51-6.

37. Li L, Liu R, Zhang Y, et al. A retrospective study on the predictive implications of clinical characteristics and therapeutic management in patients with rheumatoid arthritis-associated interstitial lung disease. *Clinical Rheumatology* 2020;39(5):1457-70.

38. Hozumi H, Nakamura Y, Johkoh T, et al. Acute exacerbation in rheumatoid arthritis-associated interstitial lung disease: a retrospective case control study. *BMJ Open* 2013;3(9):e003132.

39. Izuka S, Yamashita H, Iba A, Takahashi Y, Kaneko H. Acute exacerbation of rheumatoid arthritis–associated interstitial lung disease: clinical features and prognosis. *Rheumatology* 2021;60(5):2348-54.

40. Xiong L, Xiong L, Ye H, Ma WL. Animal models of rheumatoid arthritis-associated interstitial lung disease. *Immunity, Inflammation and Disease* 2020.

41. Sakaguchi N, Takahashi T, Hata H, et al. Altered thymic T-cell selection due to a mutation of the ZAP-70 gene causes autoimmune arthritis in mice. *Nature* 2003;426(6965):454-60.

42. Keith RC, Powers JL, Redente EF, et al. A novel model of rheumatoid arthritis-associated interstitial lung disease in SKG mice. *Exp Lung Res* 2012;38(2):55-66.

43. Deleersnijder D, Callemeyn J, Arijs I, et al. Current Methodological Challenges of Single-Cell and Single-Nucleus RNA-Sequencing in Glomerular Diseases. *Journal of the American Society of Nephrology* 2021;32(8):1838-52.

44. Slyper M, Porter CBM, Ashenberg O, et al. A single-cell and single-nucleus RNA-Seq toolbox for fresh and frozen human tumors. *Nature Medicine* 2020;26(5):792-802.

45. Ding J, Adiconis X, Simmons SK, et al. Systematic comparison of single-cell and single-nucleus RNA-sequencing methods. *Nature Biotechnology* 2020;38(6):737-46.

46. Koenitzer JR, Wu H, Atkinson JJ, Brody SL, Humphreys BD. Single-Nucleus RNA-Sequencing Profiling of Mouse Lung. Reduced Dissociation Bias and Improved Rare Cell-Type Detection Compared with Single-Cell RNA Sequencing. *Am J Respir Cell Mol Biol* 2020;63(6):739-47.

47. Korsunsky I, Millard N, Fan J, et al. Fast, sensitive and accurate integration of single-cell data with Harmony. *Nature Methods* 2019;16(12):1289-96.

48. Dovey JS, Zacharek SJ, Kim CF, Lees JA. Bmi1 is critical for lung tumorigenesis and bronchioalveolar stem cell expansion. *Proceedings of the National Academy of Sciences* 2008;105(33):11857-62.

49. Kulikauskaite J, Wack A. Teaching Old Dogs New Tricks? The Plasticity of Lung Alveolar Macrophage Subsets. *Trends in Immunology* 2020;41(10):864-77.

50. Zhang L, Wang Y, Wu G, Xiong W, Gu W, Wang C-Y. Macrophages: friend or foe in idiopathic pulmonary fibrosis? *Respiratory Research* 2018;19(1).

51. Hussell T, Bell TJ. Alveolar macrophages: plasticity in a tissue-specific context. *Nature Reviews Immunology* 2014;14(2):81-93.

52. Morse C, Tabib T, Sembrat J, et al. Proliferating SPP1/MERTK-expressing macrophages in idiopathic pulmonary fibrosis. *European Respiratory Journal* 2019;54(2):1802441.

53. Mari B, Crestani B. Dysregulated balance of lung macrophage populations in idiopathic pulmonary fibrosis revealed by single-cell RNA seq: an unstable “ménage-à-trois”. *European Respiratory Journal* 2019;54(2):1901229.

54. Woelk CH, Zhang JX, Walls L, et al. Factors regulated by interferon gamma and hypoxia-inducible factor 1A contribute to responses that protect mice from Coccidioides immitisinfection. *BMC Microbiology* 2012;12(1):218.

55. Wu H, Tang N. Stem cells in pulmonary alveolar regeneration. *Development* 2021;148(2):dev193458.

56. Ptasinski VA, Stegmayr J, Belvisi MG, Wagner DE, Murray LA. Targeting Alveolar Repair in Idiopathic Pulmonary Fibrosis. *American Journal of Respiratory Cell and Molecular Biology* 2021;65(4):347-65.

57. Katzen J, Beers MF. Contributions of alveolar epithelial cell quality control to pulmonary fibrosis. *J Clin Invest* 2020;130(10):5088-99.

58. Kulkarni T, De Andrade J, Zhou Y, Luckhardt T, Thannickal VJ. Alveolar epithelial disintegrity in pulmonary fibrosis. *American Journal of Physiology-Lung Cellular and Molecular Physiology* 2016;311(2):L185-L91.

59. Huang KY, Petretto E. Cross-species integration of single-cell RNA-seq resolved alveolar-epithelial transitional states in idiopathic pulmonary fibrosis. *Am J Physiol Lung Cell Mol Physiol* 2021;321(3):L491-L506.

60. Parimon T, Yao C, Stripp BR, Noble PW, Chen P. Alveolar Epithelial Type II Cells as Drivers of Lung Fibrosis in Idiopathic Pulmonary Fibrosis. *International Journal of Molecular Sciences* 2020;21(7):2269.

61. Treutlein B, Brownfield DG, Wu AR, et al. Reconstructing lineage hierarchies of the distal lung epithelium using single-cell RNA-seq. *Nature* 2014;509(7500):371-5.

62. Angelidis I, Simon LM, Fernandez IE, et al. An atlas of the aging lung mapped by single cell transcriptomics and deep tissue proteomics. *Nature Communications* 2019;10(1).

63. Basil MC, Katzen J, Engler AE, et al. The Cellular and Physiological Basis for Lung Repair and Regeneration: Past, Present, and Future. *Cell Stem Cell* 2020;26(4):482-502.

64. El Agha E, Kramann R, Schneider RK, et al. Mesenchymal Stem Cells in Fibrotic Disease. *Cell Stem Cell* 2017;21(2):166-77.

65. Sima, Christine, Allison, et al. Lung Stem Cell Self-Renewal Relies on BMI1-Dependent Control of Expression at Imprinted Loci. *Cell Stem Cell* 2011;9(3):272-81.

66. Distler O, Highland KB, Gahlemann M, et al. Nintedanib for Systemic Sclerosis–Associated Interstitial Lung Disease. *New England Journal of Medicine* 2019;380(26):2518-28.

67. Friedman B, Cronstein B. Methotrexate mechanism in treatment of rheumatoid arthritis. *Joint Bone Spine* 2019;86(3):301-7.

68. Cronstein BN, Sitkovsky M. Adenosine and adenosine receptors in the pathogenesis and treatment of rheumatic diseases. *Nat Rev Rheumatol* 2017;13(1):41-51.

69. Phan THG, Paliogiannis P, Nasrallah GK, et al. Emerging cellular and molecular determinants of idiopathic pulmonary fibrosis. *Cellular and Molecular Life Sciences* 2021;78(5):2031-57.

70. Philip K, Mills WT, Davies J, et al. HIF1A up-regulates the ADORA2B receptor on alternatively activated macrophages and contributes to pulmonary fibrosis. *The FASEB Journal* 2017;31(11):4745-58.

71. Zhou Y, Schneider DJ, Morschl E, et al. Distinct Roles for the A2B Adenosine Receptor in Acute and Chronic Stages of Bleomycin-Induced Lung Injury. *The Journal of Immunology* 2011;186(2):1097-106.

72. Lau CL, Beller JP, Boys JA, et al. Adenosine A2A receptor agonist (regadenoson) in human lung transplantation. *The Journal of Heart and Lung Transplantation* 2020;39(6):563-70.

73. Chunn JL, Young HWJ, Banerjee SK, Colasurdo GN, Blackburn MR. Adenosine-Dependent Airway Inflammation and Hyperresponsiveness in Partially Adenosine Deaminase-Deficient Mice. *The Journal of Immunology* 2001;167(8):4676-85.

74. Zhong H, Belardinelli L, Maa T, Zeng D. Synergy between A2BAdenosine Receptors and Hypoxia in Activating Human Lung Fibroblasts. *American Journal of Respiratory Cell and Molecular Biology* 2005;32(1):2-8.

75. Dayanim S, Lopez B, Maisonet TM, Grewal S, Londhe VA. Caffeine induces alveolar apoptosis in the hyperoxia-exposed developing mouse lung. *Pediatric Research* 2014;75(3):395-402.

76. Juge P-A, Lee JS, Lau J, et al. Methotrexate and rheumatoid arthritis associated interstitial lung disease. *European Respiratory Journal* 2021;57(2):2000337.

77. Dawson JK, Quah E, Earnshaw B, Amoasii C, Mudawi T, Spencer LG. Does methotrexate cause progressive fibrotic interstitial lung disease? A systematic review. *Rheumatology International* 2021;41(6):1055-64.

78. Saravanan V. Reducing the risk of methotrexate pneumonitis in rheumatoid arthritis. *Rheumatology* 2003;43(2):143-7.

79. Alarcon GS, Kremer JM, Macaluso M, et al. Risk factors for methotrexate-induced lung injury in patients with rheumatoid arthritis. A multicenter, case-control study. Methotrexate-Lung Study Group. *Ann Intern Med* 1997;127(5):356-64.

80. Golden MR, Katz RS, Balk RA, Golden HE. The relationship of preexisting lung disease to the development of methotrexate pneumonitis in patients with rheumatoid arthritis. *J Rheumatol* 1995;22(6):1043-7.

81. Al-Zeer MA, Al-Younes HM, Braun PR, Zerrahn J, Meyer TF. IFN-γ-Inducible Irga6 Mediates Host Resistance against Chlamydia trachomatis via Autophagy. *PLoS ONE* 2009;4(2):e4588.

82. Omura Y, Nishio Y, Takemoto T, et al. SAFB1, an RBMX-binding protein, is a newly identified regulator of hepatic SREBP-1c gene. *BMB Rep* 2009;42(4):232-7.

83. Brown PM, Pratt AG, Isaacs JD. Mechanism of action of methotrexate in rheumatoid arthritis, and the search for biomarkers. *Nature Reviews Rheumatology* 2016;12(12):731-42.

84. Nair A, Jacob S. A simple practice guide for dose conversion between animals and human. *Journal of Basic and Clinical Pharmacy* 2016;7(2):27.

85. Nagate T, Kawai J, Nakayama J. Therapeutic and Preventive Effects of Methotrexate on Zymosan-Induced Arthritis in SKG Mice. *Journal of Veterinary Medical Science* 2009;71(6):713-7.

86. Lange F. Methotrexate ameliorates T cell dependent autoimmune arthritis and encephalomyelitis but not antibody induced or fibroblast induced arthritis. *Annals of the Rheumatic Diseases* 2005;64(4):599-605.

국문 초록

서론: 류마티스 관절염 연관 간질성 폐질환 (RA-ILD)는 류마티스 관절염 환자의 사망률 증가에 기여하는 중요한 폐 외 증상 중 하나이다. 하지만 현재까지 류마티스 약물의 폐에 대한 영향을 포함한 류마티스 관절염 연관 간질성 폐질환에 대한 병태생리나 자연 경과에 대하여 잘 알려지지 않았다. 이 연구에서는 첫째 전향적 환자 코호트를 사용하여 류마티스 관절염 연관 간질성 폐질환에 대한 항류마티스 제제의 영향을 분석하고, 둘째 질환 동물 모델을 이용하여 항류마티스제제가 류마티스 관절염 연관 간질성 폐질환의 폐의 미세환경에 미치는 변화를 전사체 분석을 통해 규명하였다.

방법: 류마티스 관절염 연관 간질성 폐질환 환자의 임상경과 분석은, 코호트 분석을 위해 국내 6 개 의료기관이 참여한 한국인 류마티스 관절염 연관 간질성 폐질환 코호트 (KORAIL cohort) 데이터를 이용하여 분석하였다. 폐 섬유화 점수는 흉부 CT 검사에서 망상 혼탁 점수와 견인 기관지 확장증/기관지 확장증 점수의 합으로 정의하였다. 류마티스 관절염 연관 간질성 폐질환 질환 동물모델은 SKG 마우스를 이용하였다. 자이모산과 PBS, 자이모산과 메토트렉세이트, 자이모산과 종양 괴사인자 차단제, 그리고 아무런 투약을 하지 않은 총 4 군의 SKG 마우스의 폐 조직에서 단일핵 RNA 시퀀싱 (single nucleus RNA sequencing)을 시행하였다.

결과: 30% 이상의 폐침범을 동반한 중증 류마티스 관절염 연관 간질성 폐질환 환자에서, 폐섬유화의 점수는 2 년 및 3 년 추적에서 메토트렉세이트 치료군에서 유의하게 증가하였다. 다른 그룹과 비교하여 자이모산 A 및 메토트렉세이트 투여를 받은 SKG 마우스에서 조직학적으로 명백한 폐 염증이 관찰되었다. 자이모산 A 주입에 의한 면역 세포, 섬유아세포 및 폐포 상피 세포에서의 전사체 변화가 메토트렉세이트 투여로 더욱 강화된 반면, 종양 괴사인자 차단제 투여는 이러한 전사체 변화를 완화하여 자이모산 A 주입이 없는 SKG 마우스와 유사한 변화를 보였다. 흥미롭게도, 자이모산 A 가 투여된 마우스의 중 메토트렉세이트를 투여 받은 군의 제 II 형 폐포 세포에서 고유한 하위 세포 클러스터가 관찰되었다. 이 독특한 클러스터는 염증성 사이토 카인 자극에 의해 발현이 증가되는 유전자들이 유의하게 발현되어 있었다. 또한, 이 클러스터는 폐의 자가 재생에 필수적인 BMI1 이 결핍된 마우스와 유의하게 유사한 유전자 발현이 관찰되었다.

결론: 중증 간질성 폐질환 환자에서 메토트렉세이트 투여는 폐 섬유화를 악화시켰다. 질환 동물 모델인 자이모산 A 을 주사한 SKG 마우스에서 메토트렉세이트 투여한 개체에서도, 염증에 의한 제 II 형 폐포 세포의 재생 능력 감소로 심한 폐렴을 유발하였다.

Graphic Abstract